Sá, C., D'Alimonte, D., Brito, A. C., Kajiyama, T., Mendes, C. R., Vitorino, J., ... Brotas, V. (2015). Validation of standard and alternative satellite ocean-color chlorophyll products off Western Iberia. Remote Sensing of Environment, 168, 403–419. http://doi.org/10.1016/J.RSE.2015.07.018

Abstract

Chlorophyll a concentration (Chl) product validation off the Western Iberian coast is here undertaken by directly comparing remote sensing data with in situ surface reference values. Both standard and recently developed alternative algorithms are considered for match-up data analysis. The investigated standard products are those produced by the MERIS (algal 1 and algal 2) and MODIS (OC3M) algorithms. The alternative data products include those generated within the CoastColour Project and Ocean Color Climate Change Initiative (OC-CCI) funded by ESA, as well as a neural net model trained with field measurements collected in the Atlantic off Portugal (MLPATLP).

Statistical analyses showed that satellite Chl estimates tend to be larger than in situ reference values. The study also revealed that a non-uniform Chl distribution in the water column can be a concurring factor to thedocumented overestimation tendency when considering larger optical depth match-up stations. Among standard remote sensing products, MODIS OC3M and MERIS algal 2 yield the best agreement with in situ data. The performance of MLPATLP highlights the capability of regional solutions to further improve Chl retrieval by accounting for environmental specificities. Results also demonstrate the relevance of oceanographic regions such as the Nazaré area to evaluate how complex hydrodynamic conditions can influence the quality of Chl products.

1. Introduction

The chlorophyll *a* concentration (Chl) obtainable from satellite ocean color imagery is a key quantity for monitoring the spatial and temporal variability of the phytoplankton biomass (e.g. Behrenfeld et al., 2006; Dandonneau et al., 2004; Kahru, Kudela, Manzano-Sarabia, & Mitchell, 2012; Kahru & Mitchell, 2001; Werdell et al., 2009; Yoder, Kennelly, Doney, & Lima, 2010). During the last decades, Earth observation programs have prioritized research activities to investigate the quality of satellite data products. For instance, the space sensors of the National Aeronautics and Space Administration, NASA (e.g., Sea-Viewing Wide Field-of-View Sensor-SeaWiFS and MODerate Resolution Imaging Spectroradiometer-MODIS) and of the European Space Agency, ESA (e.g., MEdium Resolution Imaging Spectrometer-MERIS) have been validated with both geographically distributed field measurements and radiometric data collected by above-water (e.g., Zibordi et al., 2010) and moored systems (e.g. Antoine et al., 2008; Franz, Bailey, Werdell, & McClain, 2007). High-quality field measurements have also been acquired for algorithm development — e.g., the NASA bio-Optical Marine Algorithm Dataset-NOMAD (Werdell & Bailey, 2005) and the ESA MERIS MAtchup In-situ Database-MERMAID (Barker et al., 2008). Although global results tend to be within targeted uncertainties, 5% for remote sensing reflectance R_{rs} or equivalent quantities, and 35% for Chl (McClain, 2009), the comparison between primary and derived satellite data products with in situ reference values has revealed that dedicated solutions might be required to enhance applications in specific environmental regimes (e.g., Folkestad, Pettersson, & Durand, 2007; Garcia, Garcia, & McClain, 2005; Komick, Costa, & Gower, 2009; Ohde, Siegel, & Gerth, 2007; Sorensen, Aas, & Hokedal, 2007; Volpe et al., 2007).

A well-known case is represented by the use of band-ratio algorithms (e.g., Maritorena & O'Reilly, 2000; O'Reilly et al., 1998, 2000) expressing Chl as a polynomial function of R_{rs} variations in the blue-green spectral bands. The assumption that the R_{rs} band-ratio

is unequivocally related to Chl (Case 1 waters) is lessened in optically complex conditions characterized by a significant variability of Colored Dissolved Organic Material (CDOM) and/or Total Suspended Matter (TSM) with respect to phytoplankton (Case 2 waters). Validation studies have shown an overall tendency of the band-ratio approach to overestimate in situ Chl in the presence of additional CDOM and TSM with respect to their characteristic level for a certain phytoplankton amount (IOCCG, 2000). This can be explained considering that the CDOM and TSM absorptions have an exponential decay as a function of the wavelength. The presence of these optically significant substances above their standard level hence makes the R_{rs} spectral slope steeper in the blue-green range, leading the band-ratio inversion scheme to determine higher Chl values than what is in reality.

Aware of the band-ratio approach limitation, ocean color schemes have been implemented relying on neural network (NN) algorithms to utilize R_{rs} values at an extended set of individual wavelengths (e.g., Doerffer, 2011; Doerffer & Schiller, 2007). The analyses of Chl product maps (e.g., Kajiyama, D'Alimonte, & Zibordi, 2013, 2014) however indicate that NN algorithms designed for general application might still lead to suboptimal results in waters subject to specific environmental conditions (e.g., river run off, upwelling areas) and optical regimes (e.g., stratification in the vertical distribution of inherent optical properties). Optically complex Case 2 conditions, although of limited spatial extension with respect to Case 1 waters, characterize areas of utmost importance such as coastal regions of high natural biodiversity and economic value (e.g., tourism, fisheries, and aquaculture). Their monitoring is specifically required by European Union directives (e.g. Marine Strategy Framework Directive, MSFD) to limit anthropogenic pressures. Therefore quality requirements have to be established to ensure correct analysis and interpretation of ocean color data for monitoring purposes.

The importance to assess the quality of ocean-color products is also emphasized by the necessity of merging satellite observations to improve the consistency of ocean color time-series, as well as the spatial and temporal coverage of product maps applicable as Essential Climate Variable (ECV) for climate change studies. Different projects have focused on data merging to provide continuous global products, including the GlobColour project (http://www.globcolour.info), the NASA SIMBIOS Program (Fargion et al., 2003; Maritorena & Siegel, 2005), MEaSUREs projects (e.g., Maritorena, d'Andon, Mangin, & Siegel, 2010) and the recent ESA OC-CCI project (http://www.esa-oceancolour-cci.org/).

In this study a match-up analysis between in situ and satellite derived Chl is presented relying on a quality assured dataset collected in the Atlantic off Western Iberia and representative of different environmental conditions. Validation results depend on different sources of uncertainty. For instance, the quality of the in situ data is related to the measurement protocol (i.e., sampling, filtration, storage, extraction and HPLC analysis), whereas the accuracy of satellite products depend on both the performance of the atmospheric correction scheme and the ocean color inversion algorithm. Additional factors influencing comparison results are: 1) the time difference between in situ reference and satellite overpass; 2) the in situ sample being collected at surface when satellite represents the integrated Chl over the first optical depth; and 3) the satellite footprint covering area orders of magnitude larger than that captured by the in situ measurement.

The scope of this work is to document the overall quality of Chl estimates derived from different satellite sensors, bio-optical algorithms and schemes tuned for regional applications. Results are detailed accounting for environmental specificities and general guidelines are discussed for a more informed use of ocean color data products. Decomposing the overall documented differences between space-born and in situ Chl estimates into individual sources of uncertainty is however beyond the scope of this study. The specific work components are organized as follows. In Section 2 protocols for the in situ measurements and quality control criteria are described, satellite data presented, and statistical figures for match-up data analysis defined. In Section 3 results of comparisons between standard and alternative algorithms performance are presented. Specific factors affecting satellite products accuracy are considered and discussed in Section 4. Summary and conclusions are reported in Section 5.

2. Data and methods

2.1. In situ data

The in situ data considered in this study are represented by an extensive set of field measurements acquired from 2005 to 2012, mostly from early-Spring to late-Summer months, covering the North West coast of Portugal (Fig. 1), and also including samples from the Southern coast, the Gorringe bank region and the Moroccan coast.

The majority of samples were collected along the West coast of Portugal. This coastal area is generally characterized by the occurrence of seasonal upwelling, mostly observed from April to September, when northerlies favorable winds take place (Fiúza, Macedo, & Guerreiro, 1982). A band of high Chl values can usually be found in summer near the coast associated with cold nutrient-rich upwelled waters, with a strong cross-shelf gradient characterizing the separation from oceanic waters (Relvas et al., 2007). In winter, the dominant wind direction changes (westerlies and southerlies, mostly), leading to downwelling conditions and a poleward flow of relatively warm and saline water along the coast (Fiúza et al., 1982; Peliz, Dubert, Santos, Oliveira, & Le Cann, 2005; Relvas et al., 2007). However, episodes of reverse winds can occur during both periods.

In general, wind-forcing circulation interacts with the topography and the coastline structure, modifying the along-shore and cross-shelf flows at different levels, with localized and/or intensified episodes in the presence of capes or promontories (Mason, Coombs, & Oliveira, 2005). The Aveiro area is characterized by a relatively large continental shelf, which extends to the south until Nazaré, where one of the largest submarine valleys of Europe is located. The Nazaré canyon extends from the deep ocean shoreward, from 5000 m to about 150 m deep, where the canyon head is located at less than 1 km from the shore. This geomorphologic feature generates particular water circulation patterns in the area that can translate in intensified upwelling and/or sediment resuspension (Guerreiro et al., 2014 and refs therein). Along the coast, riverine input can also be a relevant source of nutrient for the phytoplankton growth. Sampling stations hence also included the Lisbon bay area, just outside the mouth of river Tagus.

Field activities were executed during two monitoring programs and on board thirteen opportunity cruises for a total of 820 water samples (Table 1). Water samples were collected using Niskin bottles mounted on a rosette, with the exception of Pelagia 2005 cruise relying on an Aquaflow pumping system. Whenever a fluorometer was available, fluorometric profiles of the water column were also conducted. The water samples were filtered through Whatman GF/F filters (nominal pore size 0.7 μm). Filters were immediately deep-frozen and stored at −80 °C and then analyzed in the laboratory for pigment identification with reversed-phase High-Performance Liquid Chromatography (HPLC).

Throughout the years, methods for sampling collection and analysis were optimized, as summarized in Table 2. In the earlier cruises, phytoplankton pigments were extracted with 95% cold-buffered methanol (2% ammonium acetate), sonicated for 1 min (Bransonic, model 1210, Hz: 47), left for 30 min at −20 °C in the dark, and finally centrifuged at 1100 *g* for 15 min at 4 °C. The samples from later cruises were extracted with 95% cold-buffered methanol (2% ammonium acetate) enriched with trans-beta-apo-8′-carotenal (i.e., internal standard) for 1 h at −20 °C, in the dark. At half-time period of extraction, samples were sonicated for 5 min, and after extraction centrifuged for 5 min. Extraction methods are discussed in Cartaxana & Brotas (2003) and Hooker et al. (2012). All extracts were filtered (Fluoropore PTFE filter membranes, 0.2 μm pore size) and immediately injected in the HPLC. Pigment extracts were analyzed using a Shimadzu HPLC comprising a solvent delivery

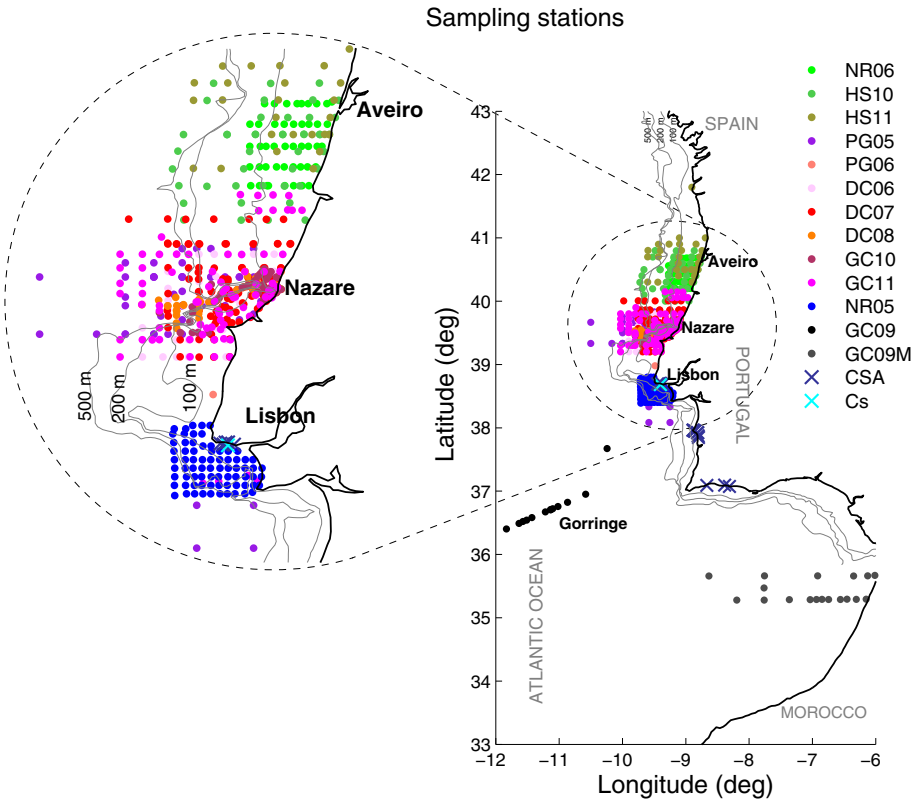

Fig. 1. The location of samples taken on board RV Pelagia in 2005 (PG05) and 2006 (PG06); NI Noruega 2005 (NR05) and 2006 (NR06); NRP D. Carlos I in 2006 (DC06), 2007 (DC07) and 2008 (DC08); NRP Gago Coutinho in 2009 (GC09 and GC09M), 2010 (GC10) and 2011 (GC11); RV Mytilus in 2010 and 2011 under HABSpot project (HS10, HS11); coastal monitoring station in Cascais (Cs) and Cascais/Sines/Algarve monitoring program (CSA).

module (LC-10ADVP) with system controller (SCL-10AVP), a photodiode array (SPD-M10ADVP), and a fluorescence detector (RF-10AXL).

Chromatographic separation in earlier cruises was performed using a C18 column for reverse phase chromatography (Supelcosil; 25 cm long; 4.6 mm in diameter; 5 μm particle size) and a 35 min elution program. The solvent gradient followed the scheme of Kraay, Zapata, and Veldhuis (1992), adapted by Brotas and Plante-Cuny (1996) with a flow rate of 0.6 mL min^{-1} and an injection volume of 100 μL. For later cruises, chromatographic separation was achieved using a C8 column for reverse phase chromatography (Symmetry C8, 15 cm long, 4.6 mm in diameter, and 3.5 μm particle size) and a 40 min elution program. The solvent gradient followed Zapata, Rodriguez, and Garrido (2000) with a flow rate of 1 mL min^{-1} and an injection volume of 100 μL. The C8 protocol allows for discriminating more pigments, namely, it separates chlorophyll c_1 from c_2, and monovinyl chlorophyll *a* from divinyl chlorophyll *a* (methods details can be found in Hooker et al., 2012; Mendes, Cartaxana, & Brotas, 2007). For all samples, pigments were identified from both absorbance spectra and retention times, and concentrations were calculated from the signals in the photodiode array detector. The HPLC system was previously calibrated with pigment standards from the Danish Hydraulic Institute (DHI) for water and environment, Denmark.

The consistency between results obtained using the C8 and the C18 columns has been assessed by: 1) applying the same quality control scheme documented below to both HPLC measurements; and 2) verifying that no systematic differences in the match-up statistical figures arise when the in situ references determined with the two chromatographic column are considered separately (details not presented).

The scheme applied for the quality control of all data pigments is that presented by Aiken et al. (2009). This scheme was used to accept or eliminate specific samples by considering the relationship between accessory pigments, AP (i.e., all carotenoids plus chlorophylls *b* and *c*) and total Chl, TChl (i.e., the sum of monovinyl chlorophyll *a*, divinyl chlorophyll *a* and chlorophyllide *a*) based on results of Trees, Clark, Bidigare, Ondrusek, and Mueller (2000) who reported that TChl is highly correlated to AP. Quality control was firstly implemented by calculating the percent difference between TChl and AP. This should be less than 30% of the total pigments concentration TPig (TChl + AP), and all samples with higher percentage differences were then eliminated from the database (i.e., a total of 50 samples were discarded, column X in Table 3). Regression analysis between TChl and AP was then applied to each cruise

Table 1
Oceanographic cruises with respective execution time, location, number of surface samples collected and Chlorophyll *a* (Chl) values range.

Cruise	Date	Location	NR of surface samples	Chl range [mg m^{-3}]
PG05	28.04.05–17.05.05	Nazaré, Lisbon	66	0.01–2.72
NR05	30.08.05–02.09.05	Lisbon bay	80	0.08–2.77
PG06	05.09.06–11.09.06	Nazaré	9	0.15–2.67
NR06	14.09.06–16.09.06	Aveiro	45	0.16–2.83
DC06	23.06.06–06.07.06	Nazaré	93	0.03–4.25
DC07	13.06.07–06.07.07	Nazaré	129	0.06–5.09
DC08	02.03.08–07.03.08	Nazaré	61	0.21–2.02
GC09_M	15.06.09–19.06.09	Morocco	21	0.01–1.70
GC09	02.06.09–05.06.09	Gorringe seamount	15	0.03–0.25
GC10	06.03.11–18.03.11	Nazaré	74	0.09–10.15
HS10	30.08.10–05.09.10	Aveiro	44	0.07–4.05
GC11	30.03.11–12.04.11	Nazaré, Lisbon, Figueira	85	0.07–1.74
HS11	09.09.11–15.09.11	Aveiro	35	0.02–2.34
Cs	03.2011–02.2012	Cascais monitoring station	45	0.13–2.74
CSA	08.2010 & 09.2011	Cascais, Sines, Algarve	18	0.26–3.57
All cruises	2005–2012	Portuguese coast; Gorringe Seamount and Morocco	820	0.01–10.15

Table 2
Sampling and processing methods applied in each cruise.

CRUISE	Sampling	Filter (type, diameter)	Filtration vol. (L)	Extraction volume (mL)	HPLC method
PG05	Aquaflow pump	GF/F, 47 mm	5	5–6	C18[a]
NR05	Niskin bottle	GF/F, 47 mm	5	5–6	C18[a]
PG06	Niskin bottle	GF/F, 47 mm	5	5–6	C18[a]
NR06	Niskin bottle	GF/F, 47 mm	5	5–6	C18[a]
DC06	Niskin bottle	GF/F, 47 mm	5	5–6	C18[a]
DC07	Niskin bottle	GF/F, 47 mm	5	5–6	C18[a]
DC08	Niskin bottle	GF/F, 47 mm	5	5–6	C18[a]
GC09_M	Niskin bottle	GF/F, 25 mm	2	2–3	C8[b]
GC09	Niskin bottle	GF/F, 25 mm	2	2–3	C8[b]
GC10	Niskin bottle	GF/F, 25 mm	2	2–3[c]	C8[b]
HS10	Niskin bottle	GF/F, 25 mm	2	2–3[c]	C8[b]
GC11	Niskin bottle	GF/F, 25 mm	2	2–3[c]	C8[b]
HS11	Niskin bottle	GF/F, 25 mm	2	2–3[c]	C8[b]
Cs	Niskin bottle	GF/F, 25 mm	1	2–3[c]	C8[b]
CSA	Niskin bottle	GF/F, 25 mm	1	2–3[c]	C8[b]

[a] Kraay et al. (1992) adapted by Brotas and Plante-Cuny (1996).
[b] Zapata et al., 2000.
[c] With internal standard.

to determine the following quality rating QR (Aiken et al., 2009): data with coefficient of determination (r^2) greater than 0.94, were given a QR = 1, else 2; root mean square error (RMS) less than 0.08, QR = 1, else 2; slope in the range 1 ± 0.1, QR = 1, else 2. Overall quality rating (OQR) was set to A* if QR = 1 for all three criteria, A if QR = 2 for any criterion, B if QR = 2 for any two criteria and C if QR = 2 for all criteria.

Quality control results are summarized in Table 3. Only one dataset was classified as C (i.e., Cs), and two cruises had A* maximum classification (i.e., PG06 and GC09). NR06, GC09_M and GC11 cruises were classified as A and the others as B. In general, the best scores were obtained by cruises with the smallest number of samples and conducted on a restricted temporal and spatial coverage (i.e., PG06 and GC09). Lower quality scores were found for the Cs monitoring program spanned throughout a year (i.e. samples from different seasonal conditions). The relationship between TChl and AP can reduce due to natural factors since the pigment composition of phytoplankton communities is highly variable and pigment proportions depend on environmental parameters such as light and nutrient availability (Ruivo, Amorim, & Cartaxana, 2011). Measurements employed for the match-up analysis were selected based on the quality control flag. The quality rating instead depends on the natural variability of quality assured data, and is reported to document the properties of the investigated area.

Following the ESA protocol (Doerffer, 2002), Chl was calculated as the sum of monovinyl chlorophyll *a*, epimers and allomers, chlorophyllide *a* and divinyl chlorophyll *a* (if C8 method was used) for the total number of samples kept after the quality control (i.e., 770 out of 820, Table 3). Chl ranged between 0.013 and 10 mg m^{-3}, which is representative of the variability range observed along the Portuguese coast throughout the year (Moita, 2001), where maximum values are found in spring/summer during upwelling events. In addition to the phytoplankton pigment analysis, a separate dataset, with both inherent and apparent optical properties (IOPs and AOPs, respectively) was collected during the GC11 cruise. This dataset was only used for the development of regional algorithms to ensure an independent assessment of match-up results.

In situ radiometric values to compute R_{rs} were measured with the microPRO free-fall optical system manufactured by Satlantic Inc. (Halifax, Canada). This instrument is equipped with radiance and irradiance multispectral sensors. Measurements to define subsurface values were collected in the near surface layer by applying the multicast technique to increase the number of samples per unit depth (D'Alimonte, Shybanov, Zibordi, & Kajiyama, 2013; D'Alimonte, Zibordi, Kajiyama, & Cunha, 2010; Zibordi, D'Alimonte, & Berthon, 2004). Radiometric products and their determination are extensively discussed in Zibordi et al. (2004), and Zibordi, Berthon, Mélin, & D'Alimonte (2011). Expected uncertainties in derived R_{rs} are ~5% in the 412–555 nm spectral range and ~6% at 665 nm.

The band-shift correction scheme (Zibordi, Mélin, & Berthon, 2006) was also applied to minimize effects of differences between in situ (λ = 412, 443, 490, 510, 555 and 665 nm) and space sensor center-

Table 3
Summary statistics of linear regression analyses between TChla and accessory pigments. Column X indicates the number of samples discarded per cruise. See text for quantities definition.

Cruise	N	X	Slope	QR	Offset	r^2	QR	RMS	QR	OQR
PG05	49	17	0.69	2	0.058	0.969	1	0.187	2	B
NR05	76	4	0.61	2	0.063	0.965	1	0.312	2	B
PG06	8	1	0.91	1	0.039	0.999	1	0.08	1	A*
NR06	45	–	1.05	1	−0.012	0.949	1	0.161	2	A
DC06	91	2	0.87	2	−0.003	0.963	1	0.189	2	B
DC07	129	–	0.70	2	0.046	0.988	1	0.232	2	B
DC08	59	2	0.60	2	0.072	0.94	1	0.247	2	B
GC09_M	19	2	0.93	1	0.012	0.998	1	0.034	2	A
GC09	15	–	0.90	1	−0.006	0.972	1	0.018	1	A*
GC10	69	5	0.67	2	0.114	0.989	1	1.002	2	B
HS10	44	–	1.15	2	0.063	0.963	1	0.354	2	B
GC11	84	1	0.94	1	0.066	0.95	1	0.101	2	A
HS11	27	8	0.65	2	0.101	0.97	1	0.454	2	B
Cs	37	8	0.84	2	0.063	0.79	2	0.308	2	C
CSA	18	–	1.18	2	−0.215	0.90	1	0.544	2	B

wavelengths (i.e., λ = 413, 443, 490, 510, 560 and 665 nm for MERIS and λ = 412, 443, 488, 530, 547 and 667 nm for MODIS). $R_{rs}(\lambda)$ values at the center wavelength λ were determined from actual $R_{rs}(\lambda_0)$ at a near center-wavelength λ_0 through

$$R_{rs}(\lambda) = R_{rs}(\lambda_0) \cdot \frac{b_b(\lambda)}{a(\lambda) + b_b(\lambda)} \cdot \frac{a(\lambda_0) + b_b(\lambda_0)}{b_b(\lambda_0)} \quad (1)$$

where a indicates the seawater absorption coefficient resulting from the sum of phytoplankton a_{phy}, non-pigmented particulate matter a_{dp}, yellow substance a_{ys}, and pure seawater a_w (Pope & Fry, 1997); and b_b is the seawater backscattering coefficient given by the sum of particle b_{bp} and pure seawater b_{bw} coefficients (Buiteveld, Hakvoort, & Donze, 1994). In situ measurements of a and b_b for the band shift correction were collected respectively with the AC-9 meter manufactured by WET Labs (Philomat, USA) and the Hydroscat-6 backscattering meter manufactured by HobiLab (Bellevue, USA). Laboratory analyses of the water samples were executed to determine the absorption coefficients by pigmented and non-pigmented particles, as well as the absorption coefficient by CDOM. It is noted that the limited number of available a_{phy} measurements did not allow for a statistical assessment of the quality of the satellite products using this parameter.

Additional in situ data collected during the GC11 cruise include measurements of beam-attenuation with the AC-9 meter; and TSM measurements performed with the dry-weight technique. Measurement protocols are detailed in Zibordi et al. (2002) and Zibordi et al. (2011).

2.2. Standard satellite data products

MODIS Aqua and MERIS Chl products (algal 1 and algal 2) were selected for the sampling area during the period of the cruises. The latest available versions of these products were used in this analysis (i.e., MODIS v.2013.1, http://oceancolor.gsfc.nasa.gov/cms/reprocessing); and MERIS 3rd reprocessing, (Bourg et al., 2011). In view of interpreting match-up validation results, it is important to acknowledge that MODIS and MERIS algal 1 algorithms were explicitly designed for open ocean, whereas MERIS algal 2 was implemented for both Case 1 and optically complex waters.

2.2.1. MODIS/AQUA OC3M algorithm

MODIS/Aqua L2 data produced by NASA Ocean Biology Processing Group (OBPG) were downloaded from the Ocean Color Website (http://oceancolor.gsfc.nasa.gov/). The applied OC3M algorithm for Chl retrieval is an extension of the OC2 and OC4 empirical algorithms developed for the SeaWiFS sensor (O'Reilly et al., 2000) to account for MODIS wavebands:

$$Chl = 10^{(0.2424 - 2.7423R + 1.8017R^2 + 0.0015R^3 - 1.2280R^4)}, \quad (2)$$

where $R = \log_{10}((R_{rs}(443) > R_{rs}(488))/R_{rs}(547))$, and R_{rs} is the remote sensing reflectance, that is the water leaving radiance (L_W) divided by the downwelling irradiance (E_s). The model parameters were derived based on NOMAD dataset, with Chl ranging from 0.012 to 72.12 mg m^{-3} (Werdell & Bailey, 2005).

2.2.2. MERIS standard algorithms

MERIS Full Resolution L2 data were provided by the ESA 3rd reprocessing completed using the MERIS Ground Segment (MEGS) Processor Version 8.0 (Bourg et al., 2011). Standard MERIS algorithms include algal 1 and algal 2 products.

2.2.2.1. MERIS algal 1. The MERIS algal 1 product is the result of a four-band polynomial algorithm OC4Me, which relates the log-transformed ratio of normalized remote sensing reflectance ρ to *Chl*. This is a semi-analytical algorithm parameterized for applications in Case 1 waters. It was developed using a theoretical ocean color model (Morel & Maritorena, 2001) tuned using K_d and Chl measurements collected by the Laboratoire d'Océanographie de Villefranche (see Antoine & Morel, 2011 for details, MERIS ATBD 2.9). Note that this approach differs from the MODIS OC3M, which is an empirical algorithm, based on the best fit of in situ data reflectance ratios and Chl. The OC4Me polynomial expression is:

$$Chl = 10^{(0.450 - 3.259R + 3.523R^2 - 3.359R^3 - 0.949R^4)} \quad (3)$$

where $R = \log_{10}((\rho(443) > \rho(490) > \rho(510))/\rho(560))$. The resulting Chl value represents the sum of monovinyl chlorophyll *a*, divinyl chlorophyll *a*, chlorophyllide *a*, and phaeophytin *a*.

2.2.2.2. MERIS algal 2. The MERIS NN algal 2 product was developed for Chl retrieval in both Case 1 and Case 2 waters. In the 3rd MERIS data reprocessing, algal 2 values are independently generated in addition to the algal 1 Chl product for Case 1 waters. The MERIS NN algorithm takes as input the logarithm of the above-surface normalized remote-sensing reflectance of MERIS bands 1–7 and 9 as well as 3 angles (solar zenith, viewing angle and azimuth difference). The output is the logarithm of 3 optical coefficients at 442 nm: 1) the scattering coefficient for all particles; 2) the sum of the absorption by CDOM and by the bleached particulate matter; and 3) the absorption by phytoplankton pigments a_{phy}, which is the difference between the absorption by the total and the bleached particulate matter (IOCCG, 2006).

The particle scattering and pigment absorption coefficients are then converted into TSM and Chl, respectively, using empirical relationships. As documented by the MERIS Product Handbook (https://earth.esa.int/pub/ESA_DOC/ENVISAT/MERIS/meris.ProductHandbook.2_1.pdf), the algal 2 product is computed as:

$$Chl = k_1 \left[a_{phy}(442)\right]^{k_2} \quad (4)$$

where $a_{phy}(442)$ (m^{-1}) is the pigment absorption at wavelength 442 nm, whereas k_1 and k_2 are empirical parameters set to 21 and 1.04, respectively, based on samples from the German Bight and Norwegian waters (Antoine et al., 2012). New empirical parameters were also calculated in this study based on samples collected during the GC11 cruise for testing regional tuning of the product ($algal2^{Reg}$).

2.2.3. Alternative algorithms

Besides standard products, a set of selected alternative algorithms was also tested. These include general inversion schemes, adaptation of standard models for regional application, and a bio-optical algorithm specifically developed for the Western Iberia area.

2.2.3.1. CoastColour. ESA has funded the CoastColour project (CC) to specifically retrieve ocean-color products accounting for coastal waters conditions. Different Chl products provided by CC were tested in this study. A first one based on an updated NN version of the MERIS algal 2 algorithm, a second one, relying on the Quasi-analytical algorithm (QAA) developed by Lee, Carder, and Arnone (2002), and a third one using the OC4 empirical algorithm. These CC algorithms benefit of a new atmospheric correction optimized for application in coastal areas, also adopting a NN approach. All rely on the same atmospheric correction scheme, but use different methods to retrieve Chl. The first two retrieve the optical absorption from the radiances measured by the MERIS sensor (i.e., NN and QAA) and then derive Chl estimates using the empirical parameterization applied in the standard algal 2 product (Eq. (4)) to convert $a_{phy}(442)$ into Chl (henceforth CC_{NN}, CC_{QAA}). Alternative testing products (i.e., CC_{NN}^{Reg} and CC_{QAA}^{Reg}) are derived in this study using the regional k_1 and k_2 parameters. The third product computes Chl directly from the radiances by applying the NASAs OC4 band ratio algorithm (CC_{OC4}). Additionally, CC also produces a merged product

by using a blending of clear water OC4 algorithm and a neural network for turbid waters, combining CC_{NN} and CC_{OC4} products, CC_{merged}. Further details on the CC algorithms and products are available at http://www.coastcolour.org/documents/Coastcolour-PUG-v2.1.pdf.

2.2.3.2. Climate Change Initiative. The Chl product delivered by the Climate Change Initiative (CCI) program is a ~4 km resolution product resulting from merged SeaWiFS, MODIS and MERIS radiometric data. The merging procedure requires a band-shift correction to account for sensor specific center bands (Zibordi et al., 2006). Processing details can be found in the Algorithm Theoretical Baseline Documents (ATBD) in the project web site http://www.esa-oceancolour-cci.org/. Once the radiometric data of the three sensors are combined, the version 6 of the OC4 algorithm (OC4v6) is used to compute the Chl values. This algorithm is an updated version of the polynomial band-ratio chlorophyll algorithm developed for SeaWiFS (O'Reilly et al., 2000), and was selected due to its historical and heritage value for climate studies. The OC4v6 uses a four-band blue-green reflectance ratio, following a revision of the algorithm in 2009 (see http://oceancolor.gsfc.nasa.gov/REPROCESSING/R2009/ocv6/ for details).

2.2.3.3. MLP for the Atlantic off Portugal. As a follow-up of former studies in different European basins (D'Alimonte, Zibordi, Berthon, Canuti, & Kajiyama, 2012; D'Alimonte, Zibordi, Kajiyama, & Berthon, 2014; Kajiyama et al., 2013, 2014), a regional Multi Layer Perceptron (MLP) neural network has been developed in this work to derive Chl from remote sensing reflectances R_{rs} using field measurements collected during the GC11 cruise. This regional MLP for the Atlantic off Portugal (ATLP) is denoted MLP_{ATLP}.

The MLP is an empirical regression scheme in principle analogous to polynomial band-ratio algorithms. The main difference between them is how regression coefficients are set. An analytical solution is available in the case of polynomial regression. The non-linearity embedded in the definition of the MLP cost function, instead, requires using numerical optimization methods during the so-called training process (Bishop, 1995).

The regional MLP_{ATLP} considered in this study was developed exclusively based on GC11 field measurements with independent R_{rs} and Chl data records to ensure separation between training samples and application cases. Notably, in situ training samples do not include any of the field measurements used for match-up analysis.

The selected MLP architecture consists of three layers of units (input, hidden and output, respectively). Multi-linear functions connect the input to the hidden units. Non-linear functions, instead, link the hidden units to the output. The number of input units is determined by the number of R_{rs} center-wavelengths. Based on previous investigations (e.g., D'Alimonte & Zibordi, 2003; D'Alimonte et al., 2012), the hidden layer is set here to ten units. In view of improving the MLP performance, both input R_{rs} and target Chl are log-transformed and z-score scaled (e.g., Bishop, 1995; Haykin, 1994; Nabney, 2001). The log-transformation is applied also considering that seawater optical properties tend to follow a log-normal distribution (Campbell, 1995). Log-transformed values are z-score scaled to generate data with mean equal to 0 and standard deviation equal to 1, which provides better numerical conditions for the MLP training (Bishop, 1995; Dransfeld, Tatnall, Robinson, & Mobley, 2006; Kajiyama, D'Alimonte, & Cunha, 2011). Radiometric data were band-shift corrected to match SeaWiFS, MODIS and MERIS bands for sensor-specific applications (Zibordi et al., 2006).

The GC11 single-cruise dataset includes a limited number of samples (i.e., 68 stations) with Chl ranging between 0.2 and 2 mg m^{-3}. This might constrain the application of the MLP_{ATLP}. Different studies have reported that regional ocean color products tend to be more accurate when derived from input R_{rs} values exhibiting statistical properties similar to those of the data used for the MLP training (D'Alimonte, Mélin, Zibordi, & Berthon, 2003; D'Alimonte et al., 2012, 2014). In fact, modeled quantities are interpolated values under these conditions. Instead, R_{rs} spectra not represented within the MLP training dataset tend to generate extrapolated results, which may be affected by larger uncertainties. The assessment of data product thus requires defining the applicability range of the regional MLP. The solution adopted in former investigations (D'Alimonte et al., 2003; Mélin et al., 2011) was to filter R_{rs} values based on the novelty detection scheme to identify application cases significantly different from those present in the training data set (Bishop, 1994). This approach is also applied in this work by considering a novelty index, henceforth denoted as η, which is based on

Table 4
Flags used for masking the satellite data.

Flag name	Description
MODIS	
ATMFAIL	Atmospheric correction failure
LAND	Pixel is over land
HIGLINT	High sun glint
HILT	Observed radiance very high or saturated
HISATZEN	High sensor view zenith angle
STRAYLIGHT	Straylight contamination is likely
CLDICE	Probable cloud or ice contamination
HISOLZEN	High solar zenith
LOWLW	Very low water-leaving radiance (cloud shadow)
CHLFAIL	Derived product algorithm failure
NAVWARN	Navigation quality is reduced
MAXAERITER	Aerosol iterations exceed maximum
CHLWARN	Derived product quality is reduced
ATMWARN	Atmospheric correction is suspect
NAVFAIL	Bad navigation
MERIS	
LAND	Pixel classified as Land in L1B, adjusted radiometrically during L2 pixel classification to allow for geocorrection errors and tidal changes.
CLOUD	Pixel classified as cloud by the L2 cloud screening algorithm (Sub-pixel, scattered cloud not includEd.)
PCD_1_13	Confidence flag for 1 to 13 (reflectances). Raised at low sun angles, when atmospheric correction fails or there are difficulties with aerosol correction. Also for pixels with whitecaps or uncorrected glint, when reflectances in any band are negative, or when reflectance at 510 nm exceeds a threshold without the turbidity flag having been raised.
PCD_15	Confidence flag for algal_1. Raised when atmospheric correction fails or there are difficulties with aerosol correction. Also for pixels with uncorrected glint or whitecaps, and for pixels with high turbidity.
PCD_17	Confidence flag for algal_2. Raised when PCD_13 is raised, or when the algorithm input or output is outside the expected range.

the Principal Component Analysis of log-transformed R_{rs} values (D'Alimonte et al., 2014). Key features of the novelty index are: 1) η is bounded between [0,∞]; 2) the more the R_{rs} spectrum is similar to the in situ measurements used for training the regional MLP, the lower is its novelty index η; 3) a R_{rs} spectrum is considered within the MLP applicability range when its η value is below a threshold; and, 4) independent analyses have shown that a threshold $\eta = 3$ fits general application requirements. Higher novelty index values (i.e., above a threshold of 3, see D'Alimonte & Zibordi, 2003; D'Alimonte et al., 2003, 2014 for details) indicate that: 1) radiometric spectral patterns are significantly different from the in situ data used for the algorithm development; and 2) corresponding MLP output values tend to be less accurate. For completeness, the MLP_{ATLP} regional algorithms were here tested considering both the entire in situ match-up database, as well as selecting samples within the MLP_{ATLP} applicability range.

2.3. Match-ups and data comparison

For the present study, MODIS data were masked with the following quality flags: land, cloud or ice, straylight, sun glint, high top of atmosphere radiance, low L_W values and specific product warning flags. The low L_W flag is used to identify cloud-shadowed pixels, or atmospheric correction failure. MERIS algal 1 and algal 2 products were masked with land, cloud and confidence flags PCD_15 and PCD_17, respectively (Table 4). Data from satellite images where the viewing angle and solar zenith angles exceeded 60° and 75°, respectively, were also excluded to avoid artifacts due to limitations of atmospheric correction algorithms at extreme viewing and solar geometries (Bailey & Werdell, 2006). For the CoastColour Chl products, L2w flags (i.e., water constituents and IOP retrieval quality flags) were applied. In the case of CCI, related products are a composite from multiple sensors combined over time (one day) and source dataset flags are not preserved. However, filtering is applied prior to the level 3 step to exclude invalid pixels (i.e., pixels where bio-optical algorithm failed, pixels not covered by MERIS, SeaWiFS or MODIS, and pixels invalid; e.g., due to land/cloud/high sun glint/atmospheric correction).

Match-ups were identified in masked satellite images of the days of in situ sampling, and satellite Chl was calculated as the mean value of the pixels within a distance of the station location of 300 m and 1 km for MERIS (and CoastColour) and MODIS, respectively. Only the data displaying a coefficient of variation (CV) lower than 25% between pixels were further considered. For CCI daily products, 3 × 3 pixel boxes were used and same criteria applied. Time differences between satellite overpass and in situ sampling were then calculated and match-ups organized per time intervals less than 3 and up to 6 h. Table 5 summarizes the spatial and satellite passage time of the different satellite products.

The following quantities were used to compare match-up data: 1) linear regression parameters including coefficient of determination (r^2), slope (A), and intercept (B); and 2) uncertainty estimates including root mean square error (Ψ), bias error (δ), and unbiased root mean square error (Δ):

$$\Psi = \sqrt{\frac{1}{N}\sum_{i=1}^{N}\left[log\left(Chl_i^{Sat}\right) - log\left(Chl_i^{Ref}\right)\right]^2} \quad (5)$$

$$\delta = \frac{1}{N}\sum_{i=1}^{N}\left[log\left(Chl_i^{Sat}\right) - log\left(Chl_i^{Ref}\right)\right] \quad (6)$$

$$\Delta = \sqrt{\frac{1}{N}\sum_{i=1}^{N}\left[\left(log\left(Chl_i^{Sat}\right) - \mu^{Sat}\right) - \left(log\left(Chl_i^{Ref}\right) - \mu^{Ref}\right)\right]^2} \quad (7)$$

where N is the total number of samples, i is the sample index, SAT indicates the satellite data, REF the reference in situ values, and $\mu^{SAT} = {}^1/_N\sum_{i=1}^{N} \log\ (Chl_i{}^{SAT})$ — analogous definition applies for μ^{REF}. Statistical analyses are presented in logarithmic scale to account for the log-normal distribution of bio-optical quantities (Campbell, 1995). Ψ was adopted to quantify the data spread (precision), and δ was selected to estimate the data offset (accuracy; i.e., residual offset remaining after positive and negative errors cancel each other). Additionally, Δ was calculated to describe the overall uncertainty of the estimated values with respect to the measured ones, regardless of the average bias (i.e., $\Psi^2 = \Delta^2 + \delta^2$).

In accordance to previous studies (Mélin et al., 2011), the mean Relative Percentage Difference (*RPD*) and the mean Absolute Percentage Difference (*APD*) were also calculated without log-transforming the Chl values:

$$RPD = \frac{1}{N}\sum_{i=1}^{N}\frac{Chl_i^{Sat} - Chl_i^{Ref}}{Chl_i^{Ref}} \times 100 \quad (8)$$

$$APD = \frac{1}{N}\sum_{i=1}^{N}\frac{\left|Chl_i^{Sat} - Chl_i^{Ref}\right|}{Chl_i^{Ref}} \times 100\,. \quad (9)$$

Linear regression parameters were computed using a Type-2 regression model, which minimizes residual variance in both x and y dimensions, rather than in the y dimension only (as in Type-1 regression).

2.4. Additional analysis based on first optical depth and euphotic depth

In addition to the statistical figures presented above, match-up results were also analyzed investigating the effect of non-uniform vertical profiles of Chl. When considering an in situ surface sample, if a deep chlorophyll maximum (DCM) occurs within the sample depth and within the layer "seen" by the remote sensor, significant biases can be introduced leading to an apparently reduced performance of the bio-optical algorithm. Although not specifically addressed here, an analogous problem can arise in the presence of inhomogeneous vertical distribution of CDOM and TSM. Validation studies should indeed consider the vertical Chl structure to calculate a weighted mean pigment concentration within the layer contributing to the radiometric signal detected by the satellite sensor (Gordon & Clark, 1980). In fact, the current MODIS Chl algorithm has been tuned to optically-weighted in situ Chl, not just surface values (Werdell & Bailey, 2005).

The surface Chl obtained by means of satellite remote sensing depends on the amount of pigment within the penetration depth (Z_{90}) defined as the water column from which 90% of the total water leaving radiance originates (Gordon & McCluney, 1975). This is generally indicated as the first optical depth (Z_{opt}), and for a homogenous ocean it can be approximated with the inverse of the diffuse attenuation coefficient ($Z_{opt} = Z_{90} \approx K_d^{-1}$).

Table 5
Spatial resolution of tested products and time of satellite overpass time.

Product	Satellite	Algorithm	Satellite overpass time (UTC)	Resolution (m)
Standard	MODIS	OC3M	~10:30	1000
	MERIS	algal 1	~13:30	300
	MERIS	algal 2	~13:30	300
Alternative	MERIS	CC_{OC4}	~13:30	300
	MERIS	CC_{NN}	~13:30	300
	MERIS	CC_{QAA}	~13:30	300
	MERIS	MLP_{ATLP}^{MER}	~13:30	300
	MODIS	MLP_{ATLP}^{MOD}	~10:30	1000
	MODIS, MERIS & SeaWiFS	CCI	12:00 (assigned)	4000

Table 6
Statistical results from the comparison between in situ and concomitant satellite data (see text for the definition of presented quantities). The match-ups analysis was performed for standard and alternative Chl products. Regional algorithms are indicated as 'Reg'. The novelty < 3 for MLP_{ATLP} algorithms indicate a threshold for the degree of novelty of the input data (D'Alimonte et al., 2014).

Product	Satellite	Algorithm	Tdiff (h)	*N*	δ	Ψ	Δ	A	B	r^2	*RPD* (%)	*APD* (%)
Standard	MODIS	OC3M	<3	26	0.153	0.267	0.218	0.78	0.03	0.74	57	68
			<6	75	0.196	0.26	0.170	0.89	0.15	0.75	67	73
	MERIS	algal 1	<3	19	0.290	0.343	0.183	0.97	0.28	0.73	111	116
			<6	35	0.279	0.34	0.194	0.98	0.27	0.73	109	111
	MERIS	algal 2	<3	35	0.07	0.321	0.313	0.87	0.03	0.42	42	62
			<6	73	0.08	0.309	0.299	1.02	0.08	0.52	49	72
Alternative	MERIS	algal 2^{Reg}	<3	35	0.108	0.359	0.343	1.31	0.16	0.42	64	82
			<6	73	0.122	0.359	0.338	1.31	0.22	0.52	79	101
	MERIS	CC_{OC4}	<3	41	0.200	0.278	0.193	0.98	0.19	0.78	80	84
			<6	83	0.18	0.301	0.242	0.95	0.16	0.64	82	92
	MERIS	CC_{merged}	<3	41	0.200	0.278	0.193	0.98	0.19	0.78	80	84
			<6	82	0.171	0.285	0.228	0.94	0.15	0.68	74	84
	MERIS	CC_{NN}	<3	29	0.139	0.249	0.206	1.38	0.23	0.85	54	65
			<6	62	0.141	0.297	0.261	1.36	0.23	0.69	67	82
		CC_{NN}^{Reg}	<3	26	0.23	0.371	0.291	1.65	0.37	0.86	110	123
	MERIS	CC_{QAA}	<3	26	0.037	0.209	0.206	1.23	0.10	0.85	22	47
			<6	55	−0.028	0.289	0.288	1.33	0.05	0.68	16	54
		CC_{QAA}^{Reg}	<3	24	0.093	0.294	0.279	1.49	0.21	0.85	53	77
	MERIS	MLP_{ATLP}^{MER}	<3	19	0.111	0.228	0.199	0.67	−0.02	0.68	41	55
		(novelty < 3)	<3	12	0.182	0.209	0.103	0.81	0.07	0.84	56	56
		MLP_{ATLP}^{MER}	<6	35	0.093	0.243	0.224	0.6	−0.07	0.63	39	57
		(novelty < 3)	<6	20	0.167	0.216	0.136	0.69	−0.00	0.82	22	56
	MODIS	MLP_{ATLP}^{MOD}	<3	26	0.105	0.261	0.239	0.62	−0.1	0.71	46	61
		(novelty < 3)	<3	11	−0.02	0.23	0.23	0.73	−0.07	0.52	6	32
		MLP_{ATLP}^{MOD}	<6	75	0.075	0.226	0.214	0.87	0.018	0.62	33	51
		(novelty < 3)	<6	46	0.05	0.189	0.182	1.18	0.1	0.61	21	38
	MODIS, MERIS & SeaWIFS	CCI	<3	139	0.245	0.331	0.222	0.75	0.12	0.74	97	105

Since this calculation was not feasible in the present study, the euphotic depth (Z_{eu}) was estimated using the surface Chl (Chl^{SURF}) as follows (Morel et al., 2007):

$$\log_{10}(Z_{eu}) = 1.524 + 0.436X - 0.0145X^2 + 0.0186X^3, \quad (10)$$

where $X = \log_{10}(Chl^{SURF})$. The euphotic depth is defined as the depth where the downwelling photosynthetic available radiation (PAR) is reduced to 1% of its value at the surface. The euphotic depth can then be related to the first optical depth, Z_{opt}:

$$Z_{opt} = \frac{Z_{eu}}{4.6}. \quad (11)$$

To understand the impact of a non-uniform vertical profile in the results, a case study was conducted. For the match-ups where the vertical fluorometric profiles were available, the optical depth (Z_{opt}) was also calculated as the inverse of Kd490 MODIS standard product. A fluorometric-integrated value *Fi* was then estimated accounting for the attenuation coefficient of light (K) within in the first optical depth (Z_{opt}) (Gordon & Clark, 1980):

$$Fi = \frac{\int_0^{Zopt} F(z)\exp(-2Kz)dz}{\int_0^{Zopt} \exp(-2Kz)dz}. \quad (12)$$

The differences between the satellite value and the surface fluorometric data, as well as the satellite value and the *Fi*-integrated result were then assessed.

3. Results

Several Chl products were tested against the correspondent in situ match-ups and summary statistics are presented in Table 6. It is remarked that match-ups were evaluated considering 3 and 6 h time-windows between satellite overpass and sample collection. The total number of samples used in each analysis was variable, even when referring to the same sensor, due to specific flags for different algorithms. For MODIS, considering a time interval of 3 h, 26 match-ups were found, and almost three times more for a 6 h time window. For MERIS, the number of match-ups ranged from 19 to 35, for a 3 h time interval, and from 35 to 73, for a 6 h time interval, for algal 1 and algal 2 products, respectively.

3.1. Satellite data vs in situ data

3.1.1. Standard chlorophyll products

When considering standard Chl products for a 3 h time window, space-born results are generally characterized by an overestimation

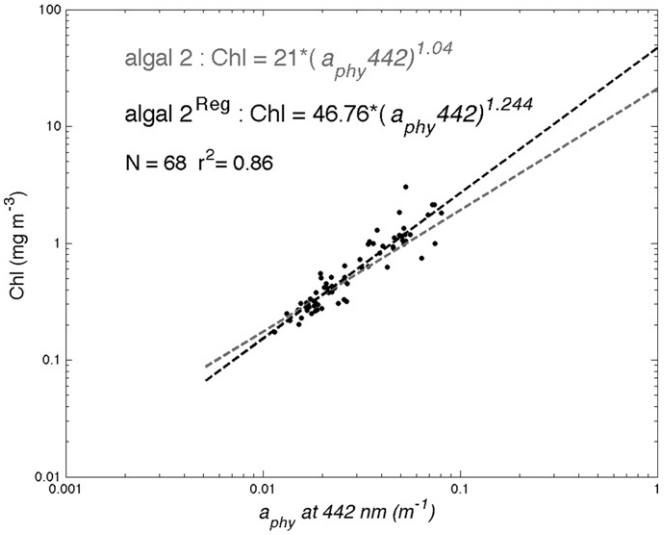

Fig. 2. Regional adjustment of the algal 2 standard product. Equation in gray is used in the algal 2 processing to convert phytoplankton absorption at 442 nm into Chl concentration. The regional adjustment was conducted using in situ data collected during GC11 cruise (black points, N = 68 and $r^2 = 0.87$). The corresponding new equation is presented in black.

with respect to the in situ measurements. The MODIS OC3M and the MERIS algal 2 algorithms yielded the best agreement with in situ HPLC data (Table 6). For instance, the bias quantified in terms of *RPD* for MODIS OC3M is 57% and 42% for algal 2 although the data dispersion for algal 2 algorithm was higher ($\Delta = 0.313$) compared to that of OC3M ($\Delta = 0.218$). Algal 1 on the other hand, yielded a *RPD* value larger than 100% (Table 6), approximately the double of that found for OC3M and algal 2.

The results obtained using a 6 h time difference were similar to those considering the 3 h time frame (Table 6). However, the number of samples increased by a factor of 3 for MODIS and a factor of ~ 2 for MERIS. The Δ value obtained for MODIS when considering 6 h difference was smaller than that for a 3 h time difference. An analogous decrease was reported for algal 2. The coefficient of determination was similar or higher for all three standard products (Table 6) when considering data fractions within 3 and 6 h.

3.1.2. Alternative Chl estimates

In situ Chl and absorption at 442 nm were used to derive a regional adaptation of the empirical parameters for the algal 2 algorithm (i.e., k_1 and k_2 of Eq. (4)) leading to a coefficient of determination of 0.86 (Fig. 2). This adjustment was performed using the GC11 cruise measurements, which included IOP and AOP data. Chlorophyll product was re-calculated based on the satellite-retrieved absorption at 442 nm, using both standard and regionally adjusted models (equations in Fig. 2). The dataset used for this regional adjustment has limited temporal and spatial coverage. The match-ups between in situ and derived Chl values revealed higher values of δ, Ψ, Δ, *RPD* and *APD* upon applying the regionalized algal 2 algorithm (see also Table 6). Thus, this regional adjustment did not improve Chl estimates with respect to the standard MERIS algal 2 values.

Comparing the CC Chl products against the in situ Chl data, the CC_{OC4} and CC_{merged} presented similar statistics (RPD 80% and APD 84%) but higher error values than the other CC products analyzed (Table 6). The CC_{NN} and CC_{QAA} products provided the best results, 54% and 22% RPD, respectively. In fact, CC_{QAA} produced better results than those obtained by the most performing standard algorithms (i.e., MODIS OC3M and MERIS algal 2). The CC_{NN} product features a similar agreement with the in situ data particularly for the *RPD* and *APD* values, as documented by algal 2 standard product (see Table 6). The CC_{NN} and CC_{QAA} algorithms developed in the CC project were also regionally adjusted (Table 6) although this did not improve the Chl retrieval as already observed in the case of the regionalized version of algal 2.

The regional MLP_{ATLP} algorithm using MERIS data as input (MLP^{MER}_{ATLP}) tends to provide Chl values in better agreement with in situ reference data when compared to the other standard products. The *RPD* and *APD* values were similar to the ones previously found for algal 2 and much lower than the ones obtained for algal 1. The coefficient of determination is also high, especially when restricting the analysis to data within the algorithm applicability range (i.e., novelty index smaller than 3, see D'Alimonte et al., 2014). The results based on an expanded 6 h time window were similar to those obtained considering only a 3 h time difference (Table 6). The number of valid pixels for this match-up analysis increased from 19 to 35 (i.e., the same as for MERIS algal 1, as input radiometric data are the same). Statistical results using the novelty threshold documented an improved agreement between the regional MLP and in situ Chl estimates.

The MLP_{ATLP} algorithm using MODIS data as input (i.e., MLP^{MOD}_{ATLP}) also yielded a better agreement with the in situ Chl when compared to the other standard algorithms evaluated in this study. Although the δ, Δ, *RPD*, *APD* and r^2 values were similar to the ones obtained using the OC3M algorithm (Table 6), restricting the analysis to the data within the MLP^{MOD}_{ATLP} applicability range, reduced both bias and scattering with respect to the in situ data. The coefficient of determination was lower than that obtained without data screening, likely due to the reduced range of variability covered by the selected samples. Considering a time interval of 6 h, the number of match-ups increased from 26 to 75 (MODIS data). Still, statistical results were similar to those obtained for a 3 h time interval.

The CCI Chl product uses satellite data from MODIS, MERIS and SeaWiFS sensors and has a spatial resolution of 4 km. The number of available match-ups ($N = 139$) is therefore much higher than that of the other algorithms (Table 6). For a time window of 3 h, the values of δ, Ψ and Δ were similar to the ones obtained for algal 1 and algal 2, and slightly higher than the equivalent results for OC3M and MLP_{ATLP}. The coefficient of determination was 0.74, i.e., within the range of values found for the standard product of MODIS and MERIS algal 1. However, relative and absolute percentage differences were approximately 100%, i.e., similar to what was obtained for algal 1, but much higher than what observed for OC3M, algal 2 and MLP_{ATLP}.

3.2. Inter-comparison between MERIS and MODIS standard products

Only 13 concomitant samples were found between MODIS and MERIS Chl products (Fig. 3a) for a 6 h time window. The statistical results of the comparison are presented in Table 7. Considering the same sub-set of match-ups, algal 2 product had the lowest RPD value 27%, indicating that MERIS algal 2 provides better results than the case-1 MODIS and MERIS products for the analyzed dataset. Algal 1 results are higher than equivalent OC3M MODIS products.

The match-ups found for both MERIS algal 1 and algal 2 products are presented in Fig. 3b. Each product depends on specific flags, only 35 valid pixels were found for this analysis for a 6 h window. Analysis based on the same subset of match-ups, shows an overestimation of algal 1 above 100%, whereas the algal 2 product is characterized by a RDP below 20%.

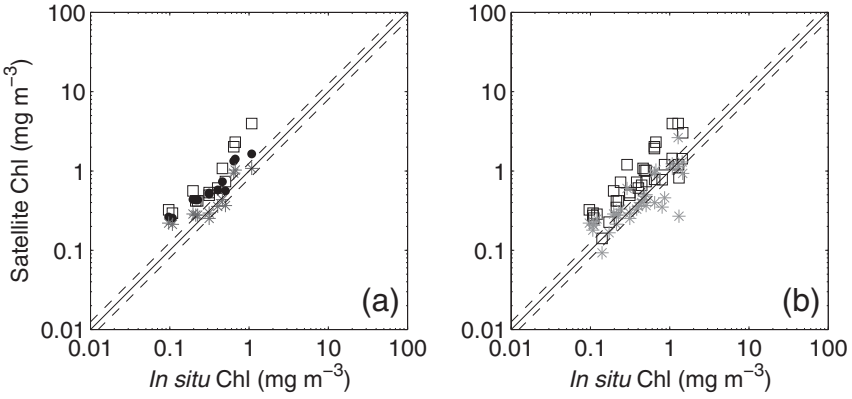

Fig. 3. Comparison of in situ Chl with satellite products for the common match-ups of MODIS OC3M (black dots), MERIS algal 1 (open squares) and algal 2 (gray asterisks) (a); as well as considering only MERIS algal 1 (open squares) and algal 2 (gray asterisks) products (b).

Table 7
Statistical results obtained using the common match-ups retrieved for different sets of standard products. The number of common match-ups is 13 for both MODIS and MERIS, and increases to 35 when considering only MERIS products (see text for the definition of presented quantities).

Product	Satellite	Algorithm	Time diff	*N*	δ	Ψ	Δ	A	B	r^2	*RPD* (%)	*APD* (%)
Standard	MODIS	OC3M	6 h	13	0.262	0.280	0.099	0.83	0.17	0.89	88	88
	MERIS	algal 1	6 h	13	0.363	0.389	0.141	1.15	0.44	0.83	143	143
		algal 2	6 h	13	0.079	0.165	0.145	0.80	−0.02	0.76	27	37
	MERIS	algal 1	6 h	35	0.279	0.34	0.194	0.98	0.27	0.73	109	111
		algal 2	6 h	35	0.020	0.216	0.215	0.83	−0.05	0.65	17	40

3.3. Overall assessment

For inter-comparison of results, the target (Jolliff et al., 2009) and Taylor (Taylor, 2001) diagrams were used to visualize statistical figures in the same summary plot. The regionalized versions of the algal 2 and CC products were not included in this analysis.

The target diagram (Fig. 4) besides providing information on Δ and δ, also allows for presenting Ψ as Euclidean distance of data points from the *x*- and *y*-axis intersection (i.e., $\Psi^2 = \Delta^2 + \delta^2$, corresponding to dotted lines in Fig. 4). In practice, the Chl products with better agreement with in situ data will appear closer to the origin.

The Taylor diagram (Fig. 5) instead summarizes the following parameters: 1) correlation coefficient, 2) standard deviation, and 3) unbiased root mean square error. Validation results are presented in the Taylor plot by using standard deviation of in situ measurements as scaling factor for the space-born match-ups. The resulting dispersion of normalized data points enables a direct inter-comparison of standard and alternative Chl estimates. The in situ reference is presented on the *x*-axis of the 2-D diagram by the standard deviation, which is normalized for the reference (i.e., the in situ data) so that this latter is equal to 1 (black star on the abscissa in Fig. 5). This allows comparing results of different algorithms represented by a point in the polar coordinate system (d, θ). The radial distance d from the origin indicates the normalized standard deviation, and the cosine of the angle θ between the direction of a data point location and the *x*-axis indicates the correlation coefficient r. The distance between the reference (i.e., black star) and the data point is, by construction, Δ (see Taylor, 2001 for further details). In analogy to the target plot, the closer a dataset point is to the reference, the more similar it is to the in situ data.

The target plots revealed that Chl products better matching with the in situ data are produced by the regionalized MLP for the Atlantic Portuguese coast. Results obtained using MODIS and MERIS radiometric inputs indicate that MLP^{MOD}_{ATLP} has low and slightly negative bias, whereas MLP^{MER}_{ATLP} has higher positive bias but smaller Δ. This might be explained by the different match-ups available for each sensor. It is also noted that these findings comply with the results presented in Fig. 3, where coincident match-ups of MODIS and MERIS reveal a higher overestimation tendency of MERIS than MODIS (analysis based on the same in situ Chl samples).

CC data products appear close to the OC3M MODIS product. Precisely, the CC_{QAA} and CC_{NN} have lower bias and outperform the CC_{OC4} version. Regarding the CCI product, this gave similar results to the standard MERIS algal 1 product, however, with more robust statistics, as the number of match-ups is higher. For the Taylor diagram, the correlation coefficients of CC products and the other algorithms is of the same order of magnitude, except for MERIS algal 2 and MLP^{MOD}_{ATLP}, that although having comparable standard deviation values, display less correlation with the in situ reference. Better results can be observed for MERIS algal 1, MODIS standard product, CC, the CCI and the MLP^{MER}_{ATLP} (the latter showing the best correlation and the smallest Δ). Data products that better approximate the variability of in situ data are those derived with the algal 1 and CC_{OC4} algorithm (i.e., the corresponding data point is that closest to the reference arc). The lower variability of MLP^{MER}_{ATLP} results ($n = 12$), when compared with that of the in situ data, can be explained by the limited set of training data used to implement this regional MLP. The difference between the standard deviations of CC_{QAA} and CC_{NN} and in situ data is comparable to that obtained by considering the other products investigated in this analysis.

3.4. Factors affecting chlorophyll product percentage error

The performance of Chl standard products was additionally evaluated through Spearman correlation analysis (Lehmann & D'Abrera, 1998) considering the total biomass, the distance of the match-ups location from the coast (D_{coast}) and the first optical depth (Z_{opt}, Section 2.4). For the MODIS match-ups, percentage error between the sensor and

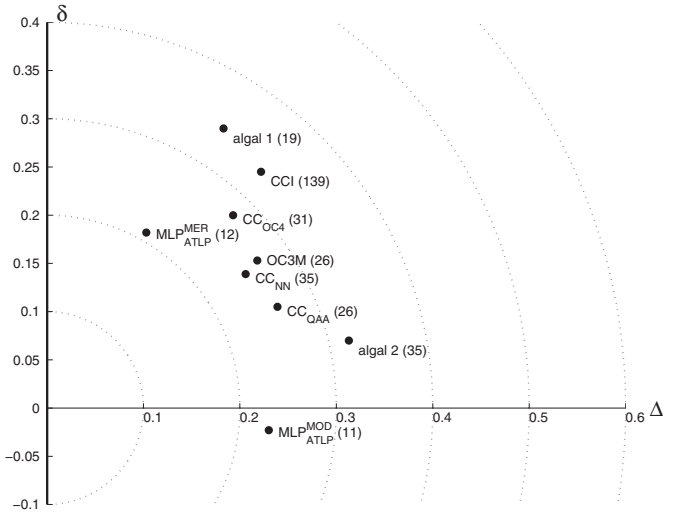

Fig. 4. Target diagram expressing the relation of Chl products with in situ match-ups. The number of match-ups is presented in parenthesis. See text for details.

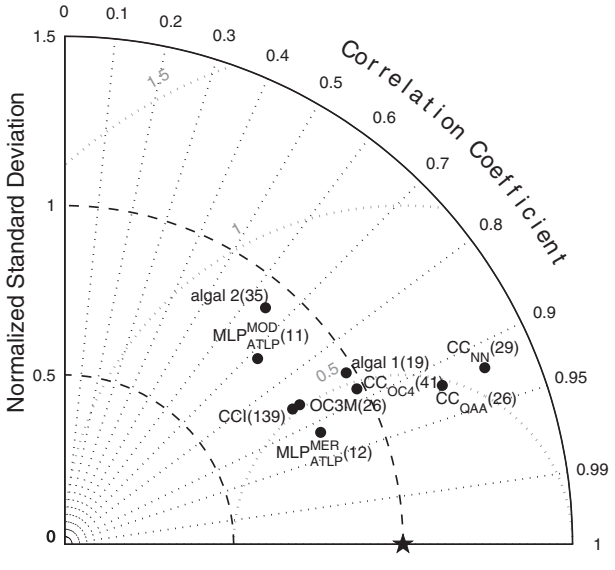

Fig. 5. As in Fig. 4, but considering the Taylor diagram.

Table 8
Correlation matrices for MODIS and MERIS standard products matchup parameters. Parameters evaluated include: percentage error between sensor and in situ data (%error), first optical depth (Zopt), distance to coast (Dcoast) and total chlorophyll a (Chl). Significative correlations appear in bold ($p < 0.05$).

MODIS OC3M	*%error*	*Zopt*	*Dcoast*	*Chl*
%error	1.00			
Zopt	**0.38**	1.00		
Dcoast	0.07	**0.53**	1.00	
Chl	−0.38	**−1.00**	**−0.53**	1.00
MERIS algal 1	*%error*	*Zopt*	*Dcoast*	*Chl*
%error	1.00			
Zopt	0.28	1.00		
Dcoast	0.31	**0.53**	1.00	
Chl	−0.28	**−1.00**	**−0.53**	1.00
MERIS algal 2	*%error*	*Zopt*	*Dcoast*	*Chl*
%error	1.00			
Zopt	**0.29**	1.00		
Dcoast	−0.14	**0.59**	1.00	
Chl	**−0.29**	−1.00	**−0.59**	1.00

the in situ data were positively correlated with Z_{opt} ($r = 0.38$, p-value < 0.05, Table 8) and negatively correlated to biomass. Biomass appeared also negatively correlated to the percentage error of MERIS algal 2 and algal 1 products, although results were only statistically significant for algal 2. For all products, match-ups Z_{opt} was significantly and positively correlated to distance from coast. Chl was instead inversely correlated to distance at a significant level for all products (Table 8). Note that the first optical depth was calculated based on the euphotic depth (Eq. (11)), which has been directly derived from surface Chl (Eq. (10)). Statistically, the optical depth was larger in the most offshore stations, which had lower biomass concentration (Table 8). Results did not display a statistically significant dependence of percentage error with the distance from coast. However, a positive tendency was observed for both MODIS and algal 1 products ($r_s = 0.07$ and $r_s = 0.31$, respectively), as opposed to a negative tendency found for the percentage error of algal 2 Chl estimates ($r_s = -0.14$).

4. Discussion

Different programs for the acquisition and processing of ocean color remote sensing data are characterized by specific features. For instance: 1) MODIS and MERIS (including CoastColour) use different atmospheric correction methods; 2) MODIS, MERIS, and CCI have different spatial scales; 3) the MODIS and MERIS L2 data have different binning scales than the level-3 4-km CCI data; and 4) the overpass time MODIS and MERIS differs by 3 h. The objective of this study is to provide an overall validation of space-borne Chl estimates in the Atlantic off the Iberian Peninsula by directly comparing in situ reference measurements with standard and alternative ocean color products. Despite a case-by-case analysis of differences between uncertainties associated with each data processing schemes goes beyond the scope of the present study, a detailed analysis of various factors affecting the comparisons is given below.

4.1. Match-ups analysis constraints

In a validation exercise, the number of match-ups available, which can vary between tested sensor and product, is crucial to guarantee the significance of statistical results. In this study, about 10% of the in situ reference samples were found to have a valid contemporaneous satellite estimate, for a 6 h time window, with the exception of CCI product. The latter, being a combination of three sensors data (i.e., SeaWiFS, MODIS and MERIS) and having 4 km of spatial resolution, had twice as much match-ups (~20%) even considering a 3 h time window. Despite the considerable number of match-ups obtained for CCI (i.e., 139), the low number of match-ups of the other Chl products (i.e., between 11 and 35) limits direct comparisons as no in situ reference sample is common to all tested products for the 3 h time window. The analysis of satellite-derived Chl accuracy is hence generally based on different in situ sample sub-sets. However, when restricting the study to selected products and considering a 6 h time window, it was possible to identify 13 coincident Chl match-ups for standard MODIS and MERIS algal 1. Likewise, 35 match-ups were identified through the direct comparison between algal 1 and algal 2 products. It is remarked that the algal 1 and algal 2 products are obtained from independent processing, which explains the different number of match-ups, considerably higher for algal 2 since it was designed also for coastal water applications.

The reduced number of match-ups considering R_{rs} measurements collected only during the GC11 cruise, limited the validation of primary radiometric quantities and therefore the assessment of the atmospheric correction impact in the Chl products uncertainty budget.

4.2. Analysis of difference between algorithms performance

Mean relative and absolute percentage differences (Table 6) revealed that both MODIS and MERIS algal 1 products overestimate in situ references, but results are significantly better for the first than for the latter. As an example, MODIS *RPD* for a 3 h time window was +57% while *RPD* for MERIS algal 1 product was +111%. This might be explained by the algorithms basis principles. For instance, MERIS algal 1 algorithm has a semi-analytical component whereas MODIS OC3M is empirically based. An independent validation exercise executed in different European seas (Zibordi, Mélin, Berthon, & Canuti, 2013) has also documented a Chl overestimation of 131% for MERIS algal 1 product in the range of approximately 0.05–20 mg m^{-3}. Similar results were also observed for algal 2. Overestimation results documented in this work for the algal 2 product are however significantly smaller (+42% for a 3 h time window).

CoastColour products also displayed different performance results despite having the same atmospheric correction. The CC_{OC4} and CC_{merged} products were very similar indicating that the merged product was mostly based on the clear-water OC4 algorithm. Both algorithms were here compared against the same in situ match-ups dataset. For CC_{NN} and CC_{QAA}, the number of match-ups retrieved was smaller, CC_{NN} having a few data points more than CC_{QAA}. These two algorithms provided better results than the CC_{OC4} indicating that algorithms suitable for coastal waters perform better in the Iberian West coast. The improved Chl agreement with the in situ data obtained for the CC_{QAA} product reveals the capability of this algorithm to better determine the phytoplankton absorption at 442 nm in comparison to CC_{NN}. This is in agreement with independent findings showing how QAA (Lee et al., 2002, 2005) and NN (algal 2, Doerffer & Schiller, 2007) provide similar results for the total absorption, but QAA gives significantly better results for the absorption of the phytoplankton and CDOM components (IOCCG, 2006). Both CC_{QAA} and CC_{NN} have been developed based on field measurements to derive inherent optical properties from the water-leaving radiances. The CC_{NN} algorithm fully relies on an empirical approach. CC_{QAA} instead is based on a semi-analytical expression of the remote sensing reflectance and uses field measurements to parameterize absorption and back-scattering components (IOCCG, 2006). The fact that CC_{QAA} embeds bio-optical principles is expected to enhance its generalization capabilities when compared to CC_{NN}.

Different algorithms performances can arise from dissimilarities between data sets besides modeling principles applied for their development. Another significant contribution can be related to the quality of bottom-of-the-atmosphere radiometry data (Cristina, Moore, Goela, Icely, & Newton, 2014). Analyses performed by Zibordi et al. (2013) indicate that the algal 1 product overestimation can also be related to the

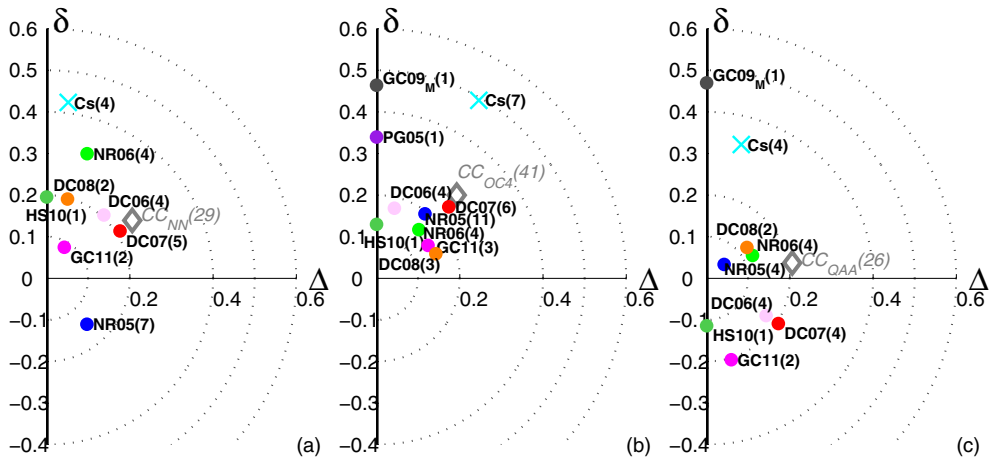

Fig. 6. Target diagram for comparison of CoastColour QAA (a) and NN (b) Chl products with their correspondent in situ match-ups. Average is presented by an open gray diamond and results obtained for each cruise are in color according to Fig. 1. The number of match-ups is presented in parenthesis.

biases between in situ and MERIS radiometric data. As an example, these authors reported a 23% underestimation of the 443/560 band-ratio for MERIS radiometric product of the 3rd MERIS data reprocessing. Besides, comparison results can also significantly change in different oceanographic regions. For instance, (Dogliotti, Schloss, Almandoz, & Gagliardini, 2009) documented a general underestimation of MODIS Chl standard product in the Patagonian Continental Shelf (i.e., −32%). Validation on a regional scale is hence required before any routine use of a satellite product in optically complex waters.

Investigation results indicate how regionally tuned schemes can allow for obtaining data products of improved quality with respect to standard space mission deliverables. An example is given by Volpe et al. (2007) in the Mediterranean Sea, where it was possible to achieve +3% of *RPD* with a dedicated empirical inversion scheme. Other case-studies were carried on by developing regional algorithm in different European Seas within ESA validation activities (D'Alimonte et al., 2014). The relevance of regional solutions for the western Iberian coast is confirmed by the present study through the analysis of results produced with the MLP_{ATLP}^{MER} algorithm characterized by low *RPD* and *APD* (Table 6). Regional MLP_{ATLP} algorithms applied to both MODIS and MERIS radiometric data tend to outperform standard satellite products. Remarkably, MLP regional products were further improved when accounting to the MLP_{ATLP} applicability range.

4.3. Specific cruise analysis

Former findings based on the overall comparison between in situ and satellite are here complemented by presenting match-ups specificities

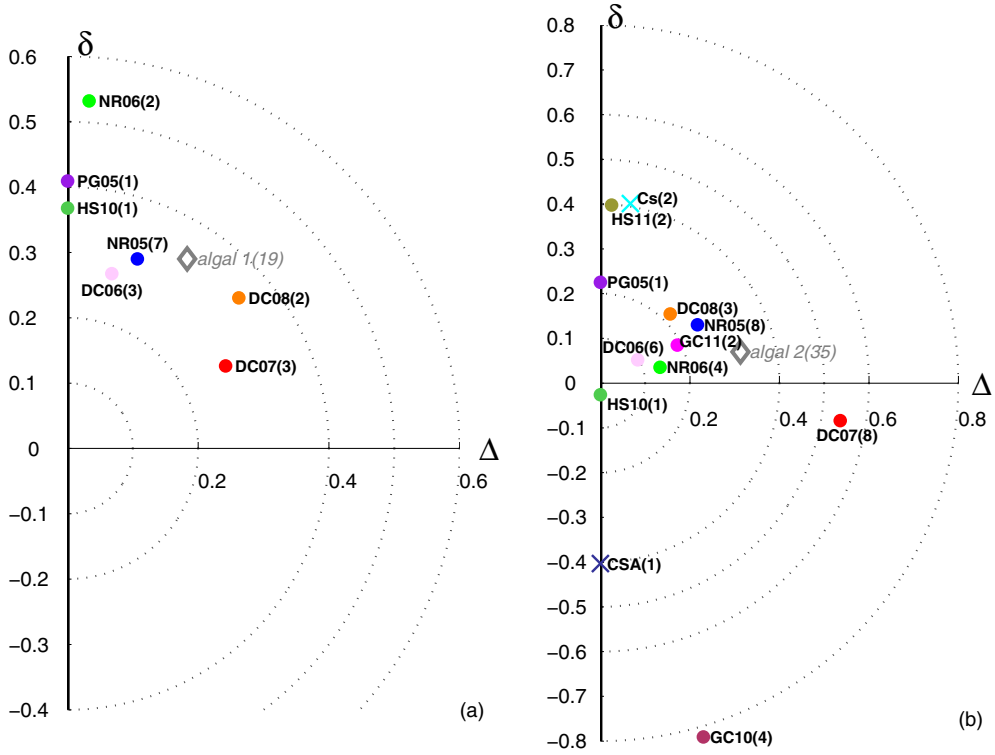

Fig. 7. As in Fig. 6, but for MERIS algal 1 and algal 2 in panels (a) and (b), respectively.

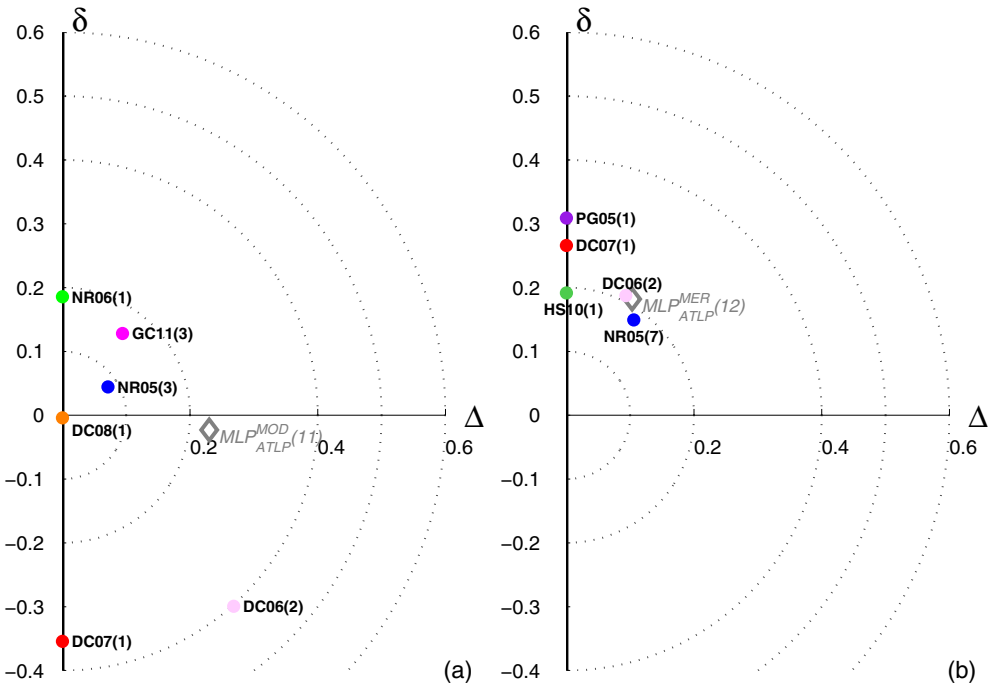

Fig. 8. As in Fig. 6, but for MLP^{MOD}_{ATLP} and MLP^{MER}_{ATLP} (novelty index < 3) in panels (a) and (b), respectively.

for each product as they correspond to different in situ reference subsets. For this purpose, target plots are used to visualize the performance of each Chl product when considering match-ups grouped by cruise. For a better interpretation of the different products tested, results are grouped as follows: 1) CC_{QAA}, CC_{NN} and CC_{OC4} in Fig. 6; 2) MERIS algal 1 and algal 2 in Fig. 7; and 3) MLP^{MER}_{ATLP} and MLP^{MOD}_{ATLP} in Fig. 8; and MODIS OC3M and CCI in Fig. 9. Figures include also data points resulting from one or two match-ups only. These results have however a limited statistical significance.

Starting with the CC, for all tested products, the samples with higher bias come from the Cs coastal monitoring station (cyan cross, Fig. 6-a-b-c). As it is a very coastal station, the atmospheric correction, which is the same for all CC products, may perform poorly in this area. Samples are also taken along the year, not in a particular season, and this variability may have also implications in the results of this station. The CC_{NN} algorithm seems to work better for the Nazaré area (pink color tone) and for the Bay of Lisbon (NR05 cruise, in blue), however, the latter with negative bias (Fig. 6-a). For CC_{OC4}, disregarding the cruises with

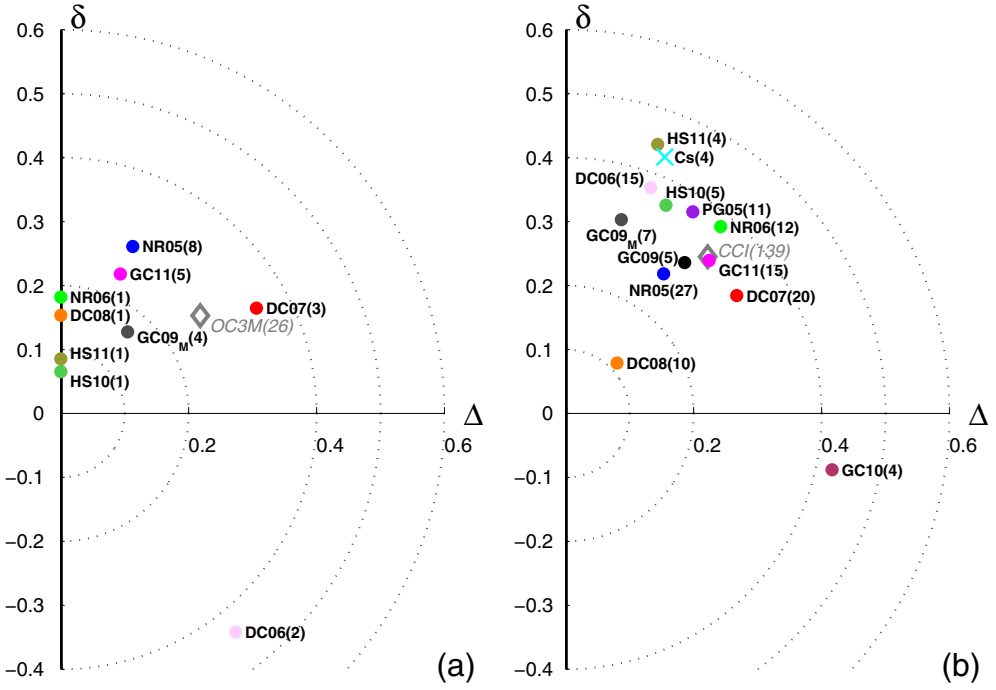

Fig. 9. As in Fig. 6, but for MODIS OC3M and CCI in panels (a) and (b), respectively.

only one match-up, and the Cs monitoring station, the product retrieved similar statistics results for all remaining match-ups. In contrast, CC_{QAA}, despite having better overall results, reveals quite good agreement in the Bay of Lisbon and Aveiro areas (NR05 and NR06 cruises) but negative bias with the match-ups from the cruises in the Nazaré area (pink color tone, i.e. cruises DC06, DC07 and GC11).

The analysis of MERIS standard algorithms shows that algal 1 performed poorly in the Aveiro area, which includes the match-ups with higher Chl values (i.e., cruises NR06 and HS10 in green, Fig. 7-a). Although, algal 2 performed very well in this oceanographic region and season, it displayed a low performance for the match-ups of the GC10 cruise (Fig. 7-b). Samples from the GC10 cruise have in situ Chl values greater than 10 mg m^{-3} due to the input of nutrients by river runoff and upwelling favorable conditions (Guerreiro et al., 2013; Martins, Vitorino, & Almeida, 2010). These samples were characterized by high phytoplankton absorption, and a phytoplankton community dominated by diatoms and coccolithophores (Brito et al., 2015; Guerreiro et al., 2013), which may explain the poor agreement for these match-ups. Despite the low performance for the samples from this cruise, the algal 2 general performance is better than algal 1 for the rest of the match-up dataset. This might depend on an improved atmospheric correction, as these algorithms rely on independent schemes.

The MLP_{ATLP}^{MER} applicability range eliminates match-ups in the Aveiro area in agreement with the limited validity of algal 1 product in this region (Fig. 8-b). MLP_{ATLP}^{MER} performs uniformly for all cruises; however the MLP_{ATLP}^{MOD} version retrieved Chl values with higher bias for the DC07 and DC06 cruises (Fig. 8-a).

MODIS OC3M, similarly to MLP_{ATLP}^{MOD}, performed poorly for the DC06 cruise, but quite well and uniformly for all the other cruises (Fig. 9-a). CCI had also uniform performances for all cruises, although underestimated Chl values reported for GC10 environmental conditions, and a particularly good agreement performance characterizes Chl estimates of the DC08 cruise (Fig. 9-b). The match-ups for this cruise correspond to a very restricted Chl range ~0.3 mg m^{-3}, likely within the optimal performance range of the algorithm.

Former examples clearly show the importance to understand how various algorithms perform in the different conditions (here represented by the considered datasets), also revealing how the overall statistics may be affected by poor performance in a specific environmental regime. Besides, this analysis gives indication of the areas of interest, where in situ sampling and analysis efforts should be directed. For instance, the different cruises conducted in the Nazaré canyon region, which displays a strong dynamical variability, revealed differences in the data product accuracy. The natural variability of this area challenges the algorithm performance, allowing for assessing the data product quality under different environmental conditions. A recent study (Mélin & Vantrepotte, 2015) has reported that intermediate regions between the coastal domain and open ocean waters, can be characterized by a high optical diversity through time. The Iberian coastal region is therein cited as an example of the bio-optical variability due to the dynamics of water masses and upwelling events. For validation purposes, these regions where temporal or spatial optical variability throughout the year is high, are preferable to obtain a validation dataset conveying the widest dynamic range of the optical variability (IOCCG, 2009).

4.4. Additional factors affecting match-up results

The first optical depth was found to be related to match-ups location, with Z_{opt} increasing with increasing distance from coast (Table 8). Closer to the coast, water turbidity is higher reducing light penetration in the water column. This implies shallower euphotic and first optical depths. Chl was also found significantly but inversely correlated to the distance from coast (D_{coast}), as well as inversely correlated to the percentage difference of all standard products. This might induce larger uncertainties in more oceanic waters, as Chl is inversely related to D_{coast}. However, results were not statistically significant in terms of direct correlation between D_{coast} and percentage difference. The percentage difference is therefore more affected by Chl and Z_{opt} and the documented low correlation can be related to two main factors: 1) low Chl concentrations can have higher measurement uncertainties; 2) Chl was only collected at the sea surface and not integrated over the water column

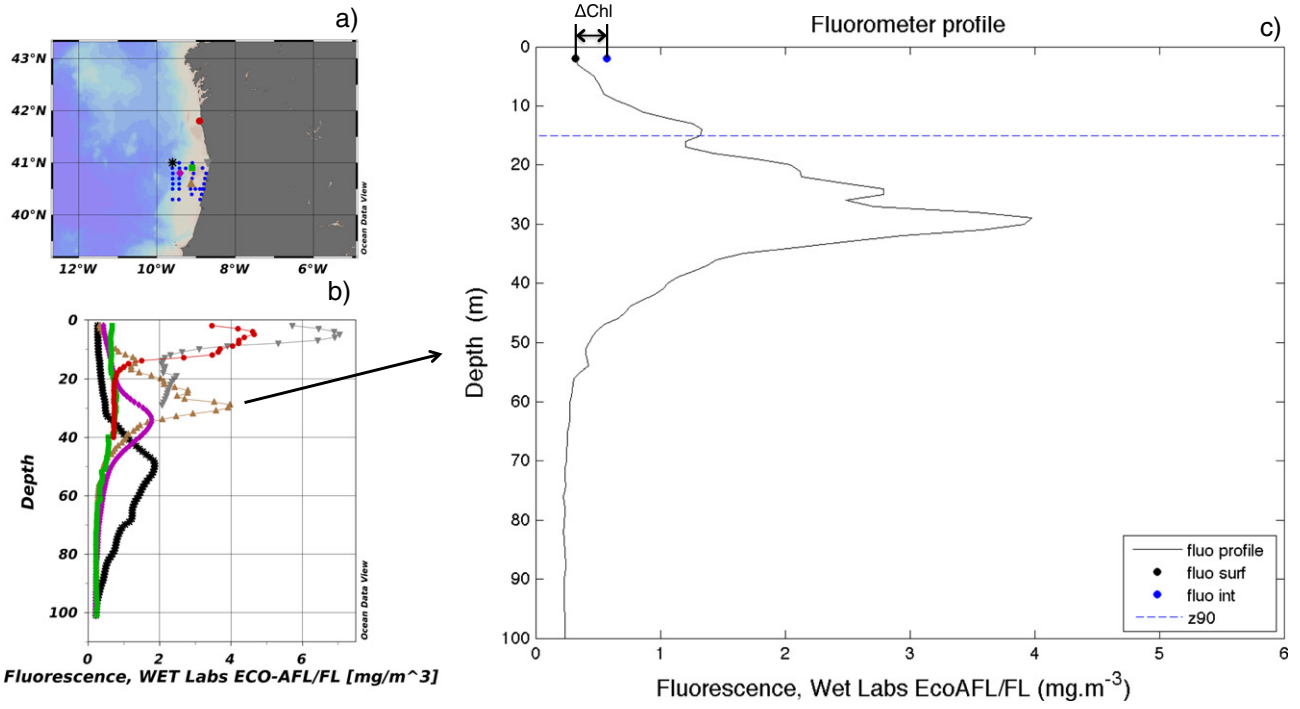

Fig. 10. a) Station locations of HS11 cruise with respective fluorometric profiles in panel b). An example of the result of integration for one of the profiles is presented in panel c).

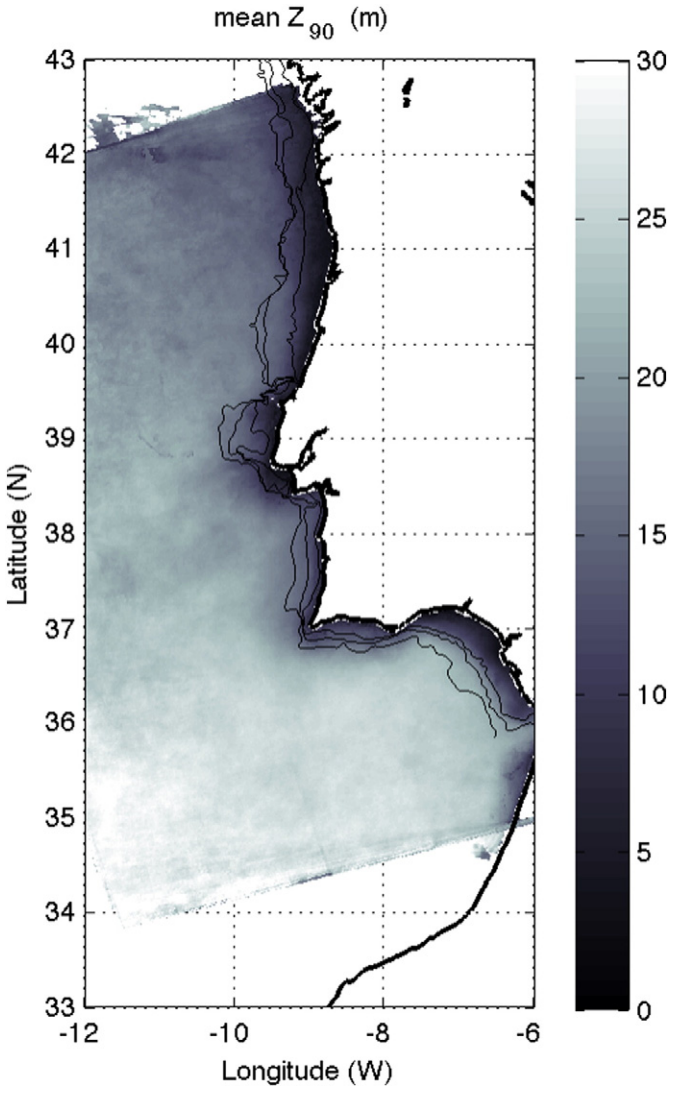

Fig. 11. Mean Z_{90} for the cruises period, calculated based on the Kd490 MODIS standard product.

to the first optical depth. In the presence of a stratified water column with a DCM, the satellite data product might then retrieve a larger Chl value than that measured at sea surface. This hypothesis has been verified by comparing Chl measured at the sea surface with the corresponding value integrated in the first optical depth, calculated based on the Kd490 MODIS standard product ($Z_{opt} = Z_{90} \approx K_d^{-1}$). Chl integration has been performed based on a limited set of fluorometric profiles and addressing the analysis to MODIS match-up data (an example is presented in Fig. 10 for the HS11 cruise). This case study has shown that the depth-integrated Chl is on average 30% larger than the value measured at the sea surface. The comparison has then been detailed by dividing the samples into two sub-groups with Z_{90} either below or above the average optical depth (i.e., 13 m). Results indicate a mean difference of 20% for the former and 40% for the latter data component. The surface Chl of these latter stations is less representative of the average Chl in the first optical depth, due to the presence of a DCM, and the larger is the optical depth the more significant becomes the effect of integration. An average map of Z_{90}, for the time of the cruises, shows larger optical depth associated with offshore waters (Fig. 11).

In agreement with the negative correlation between the Chl value and the algorithm performance documented for all standard products addressed in this study, uncertainty budgets due to a non-uniform Chl profile tend to increase at lower Chl concentrations. Note also that Stramska and Stramski (2005) reported that the contribution of a non-uniform vertical Chl profile becomes negligible when surface Chl content is greater than 0.4 mg m^{-3}, at least for deep Chl maximum (DCM) between 20 and 45 m.

5. Summary and conclusions

This work has been conducted to investigate the performance of selected Chl satellite products for the Western Iberian coast, understand their specific features and identify progress tasks. The study relied on an extensive phytoplankton pigment database, determined by HPLC analyses of water samples collected in several campaigns during the period 2005–2012. These in situ measurements, submitted to the MERMAID database under the *PortCoast* acronym, have been used here as reference to evaluate contemporaneous satellite-retrieved Chl values computed with standard (i.e., MODIS OC3M and MERIS algal 1 and algal 2) and alternative ocean-color algorithms (i.e., CC_{OC4}, CC_{QAA}, CC_{NN}, CCI and MLP_{ATLP}).

Results have shown a substantial equivalence between the performance of MODIS and MERIS algal 2 standard products (i.e., $APD = 68\%$ and 62%, respectively for a 3 h time window). It was also verified that these algorithms have better performance when compared to MERIS algal 1 ($APD = 116\%$ for the same time frame). This study has also confirmed that improvements can be achieved by coastal products (e.g. CoastColour project) and through regionalized models developed with in situ Chl and concomitant radiometric data (e.g., MLP_{ATLP}) accounting for applicability constrains, such as the novelty detection index ($APD = 32\%$ and 56% for the MODIS and MERIS version, respectively). The downside of this improvement is that regional solutions have a limited coverage area when compared to standard products.

Uncertainties affecting MODIS OC3M and algal 1 Chl have been found particularly large in comparison with the documented for algal 2. Likely because the former are based on R_{rs} values in the blue-green spectral region and the latter uses the entire set of wave bands. It should also be noticed that specific Chl definition adopted by different algorithms (e.g., MERIS algal 1 and algal 2) are not sufficient to justify the observed performance variations. The importance to account for environmental specificities on the validation results has also been discussed by considering the effect of non-uniform Chl vertical profiles. The effect of a DCM has been specifically investigated for selected match-up samples. Results indicate that in situ surface measurements may not be representative of the satellite derived Chl value, when this latter depends on the Chl distribution in the water column.

In conclusion, by demonstrating how the quality of standard products can vary in different environmental conditions, this study highlights the need of continuous assessment of space-born Chl products. Any routine use of these data for environmental monitoring of specific areas implies prior validation with in situ references. Radiometric measurements should be collected at each Chl match-up sampling station to evaluate individual sources of uncertainty (i.e., separating the contributions due to atmospheric correction and inversion schemes). Regional solutions need to be considered when application requirements are not met by standard product accuracy. In this respect, it is remarked that the complex dynamics of areas such as the Nazaré region can provide the natural variability required for testing algorithms performance in different bio-optical conditions.

It should be noted that this study represents a sensor + algorithm intercomparison. The validation program undertaken by the Marine and Environmental Sciences Centre of the University of Lisbon, MARE-UL, has been dedicated to Chl data collection. An insight from this work is the need to quantify source of uncertainties induced by the atmospheric correction process to better understand differences between in situ and space-borne Chl estimates. Radiometric field measurements currently available could only be used to assess atmospheric correction in a few cases of limited statistical validity. Work developments highlight

the need to systematically measure in situ remote sensing reflectance values for complementing seawater samples analysis. The collection of coincident radiometric data in addition to Chl measurements is also foreseen to implement regional bio-optical algorithms of better performance and increased applicability range.

Acknowledgments

The authors would like to acknowledge all people involved in the multiple sampling campaigns, namely Henko de Stigter and Teresa Moita as chief scientists of several cruises. Giuseppe Zibordi is duly acknowledged for granting the access to the radiometric data collected during the GC11 cruise. The contributions of Jean-Francois Berthon and Elisabetta Canuti during the GC11 cruise are as well recognized and acknowledged. A special thanks goes to Jean-Paul Huot for supporting the GC11 campaign. This study was performed in the framework of HabSpot FCT Project, PTDC/MAR/100348/2008 and European Space Agency projects DUE CoastColour (ESRIN/AO/1-6141/09/I-EC) and Climate Change Iniciative — Ocean Color (AO-1/6207/09/I-LG). The work has been also partially supported by the European Space Agency within the framework of the MERIS Validation Activities under contract n. 12595/09/I-OL, and sampling activities benefited from European projects HERMES (GOCE-CT-2005-511234) and Hermione (EC contract 226354) support. We would like to thank NASA OBPG for the MODIS data and ESA Project AOPT-2423 for providing MERIS full resolution images. Carolina Sá received a grant from the Portuguese Science Foundation (FCT-SFRH/BD/24245/2005). Ana C. Brito was funded by a Portuguese Post-doc grant from FCT (BPD/63017/2009) and by the Investigador FCT Program (IF/00331/2013). Davide D'Alimonte was funded by Investigador FCT Program (IF/00541/2013). Carlos R. Mendes was funded by a Pos-doc grant from CAPES (Brazil). Three anonymous reviewers are duly acknowledged for their comments very helpful to improve this study.

References

Aiken, J., Pradhan, Y., Barlow, R., Lavender, S., Poulton, A., Holligan, P., et al. (2009). Phytoplankton pigments and functional types in the Atlantic Ocean: A decadal assessment, 1995–2005. *Deep-Sea Research Part II*, *56*(15), 899–917 (The Atlantic Meridional Transect Program).

Antoine, D., Bourg, L., Brockmann, C., Doerffer, R., Fischer, J., Moore, J., Santer, R., & Zagolski, F. (2012). *Reference Model for MERIS Level 2 Processing – Third MERIS reprocessing: Ocean Branch, Report n. PO-TN-MEL-GS-0026-5 Rev. 2.* available at: http://envisat.esa.int/instruments/meris/rfm/, 106 pp.

Antoine, D., d'Ortenzio, F., Hooker, S.B., Bécu, G., Gentili, B., Tailliez, D., et al. (2008). Assessment of uncertainty in the ocean reflectance determined by three satellite ocean color sensors (MERIS, SeaWiFS and MODIS-A) at an offshore site in the Mediterranean Sea (BOUSSOLE project). *Journal of Geophysical Research, Oceans*, *113*(C7).

Antoine, D., & Morel, A. (2011). *MERIS Algorithm Theoretical Basis Document (ATBD) 2.7 — Atmospheric correction of the MERIS observations over ocean case 1 waters.*

Bailey, S.W., & Werdell, P.J. (2006). A multi-sensor approach for the on-orbit validation of ocean color satellite data products. *Remote Sensing of Environment*, *102*, 12–23.

Barker, K., Mazeran, C., Lerebourg, C., Bouvet, M., Antoine, D., Ondrusek, M., et al. (2008). MERMAID: The MERis MAtchup In-situ Database. *Proceedings of the 2nd (A)ATSR and MERIS workshop, Frascati, Italy. ESA/ESRIN.*

Behrenfeld, M.J., ÓMalley, R.T., Siegel, D.A., McClain, C.R., Sarmiento, J.L., Feldman, G.C., et al. (2006). Climate-driven trends in contemporary ocean productivity. *Nature*, *444*(7120), 752–755.

Bishop, C.M. (1994). Novelty detection and neural network validation. *IEE Proceeding Vision and Image & Signal Processing*, *141*, 217–222.

Bishop, C.M. (1995). *Neural networks for pattern recognition.* Oxford University Press.

Bourg, L., Lerebourg, C., Mazeran, C., Bruniquel, V., Barker, K., Jackson, J., et al. (2011). Meris 3rd data reprocessing: Software and adf updates. *Technical report, Report n. A879.NT.008.ACRI-ST, 21091/07/I-OL* (73 pp.).

Brito, A.C., Sá, C., Brotas, V., Brewin, R.J.W., Silva, T., Vitorino, J., et al. (2015). Effect of phytoplankton size classes on bio-optical properties of phytoplankton in the Western Iberian coast: Application of models. *Remote Sensing of Environment*, *156*, 537–550.

Brotas, V., & Plante-Cuny, M. (1996). Identification et quantification des pigments chlorophylliens et caroténoides • des sédiments marins: un protocole d'analyse par HPLC. *Oceanologica Acta*, *19*, 623–634.

Buiteveld, H., Hakvoort, J.H.M., & Donze, M. (1994). The optical properties of pure water. *Ocean Optics XII, Vol. 2258.* (pp. 174–183). SPIE.

Campbell, J.W. (1995). The lognormal distribution as a model for the bio-optical variability in the sea. *Journal of Geophysical Research*, *100*, 237–254.

Cartaxana, P., & Brotas, V. (2003). Effects of extraction on HPLC quantification of major pigments from benthic microalgae. *Archives für Hydrobiologie*, *157*(3), 339–349.

Cristina, S., Moore, G., Goela, P., Icely, J., & Newton, A. (2014). In situ validation of MERIS reflectance off the SW Iberian Peninsula: assessment of various adjustment and corrections for near-land adjacency. *International Journal of Remote Sensing*, *35*(6), 1–31.

D'Alimonte, D., Mélin, F., Zibordi, G., & Berthon, J. -F. (2003). Use of the novelty detection technique to identify the range of applicability of empirical ocean colour algorithms. *IEEE Transactions on Geoscience and Remote Sensing*, *41*, 2833–2843.

D'Alimonte, D., Shybanov, E.B., Zibordi, G., & Kajiyama, T. (2013). Regression of in-water radiometric profile data. *Optics Express*, *21*(23), 27.

D'Alimonte, D., & Zibordi, G. (2003). Phytoplankton determination in an optically complex coastal region using a multilayer perceptron neural network. *IEEE Transactions on Geoscience and Remote Sensing*, *41*(12), 2861–2868.

D'Alimonte, D., Zibordi, G., Berthon, J. -F., Canuti, E., & Kajiyama, T. (2012). Performance and applicability of bio-optical algorithms in different European seas. *Remote Sensing of Environment*, *124*, 402–412.

D'Alimonte, D., Zibordi, G., Kajiyama, T., & Berthon, J. -F. (2014). Comparison between MERIS and regional high-level products in European seas. *Remote Sensing of Environment*, *140*, 378–395.

D'Alimonte, D., Zibordi, G., Kajiyama, T., & Cunha, J.C. (2010). Monte Carlo code for high spatial resolution ocean color simulations. *Applied Optics*, *49*(26), 4936–4950.

Dandonneau, Y., Deschamps, P. -Y., Nicolas, J. -M., Loisel, H., Blanchot, J., Montel, Y., et al. (2004). Seasonal and interannual variability of ocean color and composition of phytoplankton communities in the north atlantic, equatorial pacific and south pacific. *Deep-Sea Research Part II*, *51*, 303–318.

Doerffer, R. (2002). Protocols for the validation of MERIS water products. *Technical report, European Space Agency. Doc. No. PO-TN-MEL-GS-0043.*

Doerffer, R. (2011). *MERIS Algorithm Theoretical Basis Document (ATBD) 2.25 — Alternative atmospheric correction procedure for case 2 water remote sensing using MERIS.*

Doerffer, R., & Schiller, H. (2007). The MERIS Case 2 water algorithm. *International Journal of Remote Sensing*, *28*(3–4), 517–535.

Dogliotti, A.I., Schloss, I.R., Almandoz, G.O., & Gagliardini, D.A. (2009). Evaluation of SeaWiFS and MODIS chlorophyll? A products in the Argentinean Patagonian Continental Shelf (38°S–55°S). *International Journal of Remote Sensing*, *30*(1), 251–273.

Dransfeld, S., Tatnall, A., Robinson, I., & Mobley, C. (2006). Neural network training: Using untransformed or log-transformed training data for the inversion of ocean colour spectra? *International Journal of Remote Sensing*, *27*(10), 2011–2016 (cited By (since 1996) 1).

Fargion, G., Franz, B., Kwiatkowska, E., Pietras, C., Bailey, S., Gales, J., et al. (2003). Simbios program in support of ocean color missions: 1997–2003. *Proc. SPIE Int. Soc. Opt. Eng. Vol. 5155.* (pp. 49–60).

Fiúza, A.F.G., Macedo, M.E., & Guerreiro, M.R. (1982). Climatological space and time variation of the Portuguese coastal upwelling. *Oceanologica Acta*, *5*, 31–40.

Folkestad, A., Pettersson, L.H., & Durand, D.D. (2007). Inter-comparison of ocean colour data products during algal blooms in the skagerrak. *International Journal of Remote Sensing*, *28*(3–4), 569–592.

Franz, B.A., Bailey, S.W., Werdell, P.J., & McClain, C.R. (2007). Sensor-independent approach to the vicarious calibration of satellite ocean color radiometry. *Applied Optics*, *46*(22), 5068–5082.

Garcia, C.A.E., Garcia, V.M.T., & McClain, C.R. (2005). Evaluation of SeaWiFS chlorophyll algorithms in the Southwestern Atlantic and Southern Oceans. *Remote Sensing of Environment*, *95*(1), 125–137.

Gordon, H.R., & Clark, D.K. (1980). Remote sensing optical properties of a stratified ocean: An improved interpretation. *Applied Optics*, *19*, 3428–3430.

Gordon, H.R., & McCluney, W.R. (1975). Estimation of the depth of sunlight penetration in the sea for remote sensing. *Applied Optics*, *14*, 413–416.

Guerreiro, C., Oliveira, A., de Stigter, H., Cachão, M., SC, Borges, C., et al. (2013). Late winter coccolithophore bloom off central Portugal in response to river discharge and upwelling. *Continental Shelf Research*, *59*, 65–83.

Guerreiro, C., Sá, C., de Stigter, H., Oliveira, A., Cachão, M., Cros, L., et al. (2014). Influence of the Nazaré Canyon, central Portuguese margin, on late winter coccolithophore assemblages. *Deep-Sea Research Part II*, *104*, 335–358.

Haykin, S. (1994). *Neural networks: A comprehensive foundation.* New York: Macmillan.

Hooker, S., Clementson, L., Thomas, C., Schlüter, L., Allerup, M., Ras, J., et al. (2012). *The Fifth SeaWiFS HPLC Analysis Round-Robin Experiment (SeaHARRE-5).* NASA tech. memo. 2012-217503. Greenbelt, Maryland: NASA Goddard Space Flight Center.

IOCCG (2000). Remote sensing of ocean colour in coastal, and other optically-complex, waters. In S. Sathyendranath (Ed.), *Reports of the International Ocean-Colour Coordinating Group. Number 3.* Dartmouth, Canada: IOCCG, IOCCG.

IOCCG (2006). Remote sensing of inherent optical properties: Fundamentals, tests of algorithms, and applications. In Z. -P. Lee (Ed.), *Reports of the International Ocean-Colour Coordinating Group. Number 5.* Dartmouth, Canada: IOCCG.

IOCCG (2009). Partition of the ocean into ecological provinces: Role of ocean-colour radiometry. In M. Dowell, & T. Platt (Eds.), *Reports of the International Ocean-Colour Coordinating Group. Number 9.* Dartmouth, Canada: IOCCG.

Jolliff, J.K., Kindle, J.C., Shulman, I., Penta, B., Friedrichs, M.A., Helber, R., et al. (2009). Summary diagrams for coupled hydrodynamic-ecosystem model skill assessment. *Journal of Marine Systems*, *76*, 64–82.

Kahru, M., Kudela, R.M., Manzano-Sarabia, M., & Mitchell, B.G. (2012). Trends in the surface chlorophyll of the California current: Merging data from multiple ocean color satellites. *Deep-Sea Research Part II*, *77–80*, 89–98.

Kahru, M., & Mitchell, B.G. (2001). Seasonal and nonseasonal variability of satellite derived chlorophyll and coloured dissolved organic matter concentration in the California current. *Journal of Geophysical Research*, *106*, 2517–2529.

Kajiyama, T., D'Alimonte, D., & Cunha, J.C. (2011). Performance prediction of ocean color Monte Carlo simulations using multi-layer perceptron neural networks. *Procedia Computer Science, Vol. 4.* (pp. 2186–2195) (Singapore). Proceedings of the International Conference on Computational Science, ICCS 2011. Available: http://dx.doi.org/10.1016/j.procs.2011.04.239.

Kajiyama, T., D'Alimonte, D., & Zibordi, G. (2013). Regional algorithms for European seas: A case study based on MERIS data. *IEEE Geoscience and Remote Sensing Letters*, *10*(2), 283–287.

Kajiyama, T., D'Alimonte, D., & Zibordi, G. (2014). Match-up analysis of MERIS radiometric data in the Northern Adriatic Sea. *IEEE Geoscience and Remote Sensing Letters*, *11*(1), 19–23.

Komick, N., Costa, M., & Gower, J. (2009). Bio-optical algorithm evaluation for {MODIS} for western Canada coastal waters: An exploratory approach using in situ reflectance. *Remote Sensing of Environment*, *113*(4), 794–804.

Kraay, G.W., Zapata, M., & Veldhuis, M.J.W. (1992). Separation of chlorophylls c1c2, and c3 of marine phytoplankton by reversed-phase-c18-high-performance liquid chromatography1. *Journal of Phycology*, *28*(5), 708–712.

Lee, Z., Carder, K.L., & Arnone, R.A. (2002). Deriving inherent optical properties from water color: A multiband quasi-analytical algorithm for optically deep waters. *Applied Optics*, *41*(27), 5755–5772.

Lee, Z. -P., Darecki, M., Carder, K.L., Davis, C.O., Stramski, D., & Rhea, W.J. (2005). Diffuse attenuation coefficient of downwelling irradiance: An evaluation of remote sensing methods. *Journal of Geophysical Research, Oceans*, *110*(C2) (n/a–n/a).

Lehmann, E.L., & D'Abrera, H.J.M. (1998). *Nonparametrics: Statistical methods based on ranks.* NJ: Prentice-Hall.

Maritorena, S., d'Andon, O.H.F., Mangin, A., & Siegel, D.A. (2010). Merged satellite ocean color data products using a bio-optical model: Characteristics, benefits and issues. *Remote Sensing of Environment*, *114*(8), 1791–1804.

Maritorena, S., & O'Reilly, J.E. (2000). *OC2v2: Update on the initial operational SeaWiFS chlorophyll-a algorithm*, volume 11 of *SeaWiFS postlaunch Technical Report SERIES*. Greenbelt, MD: NASA Goddard Space Flight Center, TM-2000-206892.

Maritorena, S., & Siegel, D.A. (2005). Consistent merging of satellite ocean color data sets using a bio-optical model. *Remote Sensing of Environment*, *94*(4), 429–440.

Martins, I., Vitorino, J., & Almeida, S. (2010). The Nazaré Canyon observatory (W Portugal) real-time monitoring of a large submarine canyon. *OCEANS 2010 IEEE* (pp. 1–7). Sydney, NSW: IEEE.

Mason, E., Coombs, S., & Oliveira, P.B. (2005). *An overview of the literature concerning the oceanography of the eastern North Atlantic region. Relat. Cient. Téc. IPIMAR, Série digital n°33* (58 pp. (available at https://www.ipma.pt/resources.www/docs/publicacoes.site/docweb/2006/Reln33final.pdf)).

McClain, C.R. (2009). A decade of satellite ocean color observation. *Annual Review of Marine Science*, *1*, 19–42.

Mélin, F., & Vantrepotte, V. (2015). How optically diverse is the coastal ocean? *Remote Sensing of Environment*, *160*, 235–251.

Mélin, F., Vantrepotte, V., Clerici, M., D'Alimonte, D., Zibordi, G., Berthon, J.F., et al. (2011). Multi-sensor satellite time series of optical properties and chlorophyll-a concentration in the Adriatic Sea. *Progress in Oceanography*, *91*(3), 229–244.

Mendes, C.R., Cartaxana, P., & Brotas, V. (2007). HPLC determination of phytoplankton and microphytobenthos pigments: Comparing resolution and sensitivity of a C_{18} and a C_8 method. *Limnology and Oceanography: Methods*, *5*, 363–370.

Moita, M. (2001). *Structure, variability and dynamics of phytoplankton from the Portuguese continental coast.* (Phd dissertation) Lisbon: University of Lisbon.

Morel, A., Huot, Y., Gentili, B., Werdell, P.J., Hooker, S.B., & Franz, B.A. (2007). Examining the consistency of products derived from various ocean color sensors in open ocean (case 1) waters in the perspective of a multi-sensor approach. *Remote Sensing of Environment*, *111*(1), 69–88.

Morel, A., & Maritorena, S. (2001). Bio-optical properties of oceanic waters: A reappraisal. *Journal of Geophysical Research*, *106*(C4), 7163–7180.

Nabney, I.T. (2001). *Netlab: Algorithms for pattern recognition.* London: Springer-Verlag.

O'Reilly, J.E., Maritorena, S., Mitchell, B.G., Siegel, D.A., Carder, K.L., Garver, S.A., et al. (1998). Ocean color chlorophyll algorithms for SeaWiFS. *Journal of Geophysical Research*, *103*, 24937–24953.

O'Reilly, J.E., Maritorena, S., Siegel, D.A., O'Brien, M.C., Toole, D., Mitchell, B.G., et al. (2000). *Ocean color chlorophyll a algorithms for SeaWiFS, OC2, OC4: Version 4*, volume 11 of *SeaWiFS postlaunch technical report series*. Greenbelt, Maryland: NASA/TM-1995-104566, NASA Goddard Space Flight Center.

Ohde, T., Siegel, H., & Gerth, M. (2007). Validation of Meris level-2 products in the Baltic Sea, the Namibian coastal area and the Atlantic Ocean. *International Journal of Remote Sensing*, *28*(3–4), 609–624.

Peliz, A., Dubert, J., Santos, A.M.P., Oliveira, P.B., & Le Cann, B. (2005). Winter upper ocean circulation in the Western Iberian Basin — Fronts, Eddies and Poleward flows: An overview. *Deep Sea Research, Part I*, *52*, 621–646.

Pope, R.M., & Fry, E.S. (1997). Absorption spectrum (380–700 nm) of pure water: II. Integrating cavity measurements. *Applied Optics*, *36*, 8710–8723.

Relvas, P., Barton, E.D., Dubert, J., Oliveira, P.B., Peliz, A., da Silva, J.C.B., et al. (2007). Physical oceanography of the western Iberia ecosystem: Latest views and challenges. *Progress in Oceanography*, *74*, 149–173.

Ruivo, M., Amorim, A., & Cartaxana, P. (2011). Effects of growth phase and irradiance on phytoplankton pigment ratios: Implications for chemotaxonomy in coastal waters. *Journal of Plankton Research*, *33*(7), 1012–1022.

Sorensen, K., Aas, E., & Hokedal, J. (2007). Validation of MERIS water products and bio-optical relationships in the Skagerrak. *International Journal of Remote Sensing*, *28*, 555–568.

Stramska, M., & Stramski, D. (2005). Effects of a nonuniform vertical profile of chlorophyll concentration on remote-sensing reflectance of the ocean. *Applied Optics*, *44*, 1735–1747.

Taylor, K.E. (2001). Summarizing multiple aspects of model performance in a single diagram. *Journal of Geophysical Research — Atmospheres*, *106*(D7), 7183–7192.

Trees, C.C., Clark, D.K., Bidigare, R.R., Ondrusek, M.E., & Mueller, J.L. (2000). Accessory pigments versus chlorophyll a concentration within the euphotic zone: An ubiquitous relationship. *Limnology and Oceanography*, *45*, 1130–1143.

Volpe, G., Santoleri, R., Vellucci, V., d'Alcalà, M.R., Marullo, S., & D'Ortenzio, F. (2007). The colour of the Mediterranean Sea: Global versus regional bio-optical algorithms evaluation and implication for satellite chlorophyll estimates. *Remote Sensing of Environment*, *107*(4), 625–638.

Werdell, P.J., & Bailey, S.W. (2005). An improved in-situ bio-optical data set for ocean color algorithm development and satellite data product validation. *Remote Sensing of Environment*, *98*, 122–140.

Werdell, P.J., Bailey, S.W., Franz, B.A., Jr., L. W. H., Feldman, G.C., & McClain, C.R. (2009). Regional and seasonal variability of chlorophyll-a in Chesapeake Bay as observed by SeaWiFS and MODIS-Aqua. *Remote Sensing of Environment*, *113*(6), 1319–1330.

Yoder, J., Kennelly, M., Doney, S., & Lima, I. (2010). Are trends in SeaWiFS chlorophyll time-series unusual relative to historic variability. *Acta Oceanologica Sinica*, *29*(2), 1–4.

Zapata, M., Rodriguez, F., & Garrido, J. (2000). Separation of chlorophylls and carotenoids from marine phytoplankton: A new hplc method using a reversed phase c8 column and pyridine-containing mobile phases. *Marine Ecology Progress Series*, *195*, 29–45.

Zibordi, G., Berthon, J. -F., Doyle, J.P., Grossi, S., van der Linde, D., Targa, C., et al. (2002). *Coastal Atmosphere and Sea Time SERIES (CoASTS): A long-term measurement program*, volume 19 of *SeaWiFS postlaunch Technical Report SERIES*. Greenbelt, MD: NASA Goddard Space Flight Center, TM-2001-206892.

Zibordi, G., Berthon, J. -F., Mélin, F., & D'Alimonte, D. (2011). Cross-site consistent in situ measurements for satellite ocean color applications: The BiOMaP radiometric dataset. *Remote Sensing of Environment*, *115*(8), 2104–2115.

Zibordi, G., D'Alimonte, D., & Berthon, J. -F. (2004). An evaluation of depth resolution requirements for optical profiling in coastal waters. *Journal of Atmospheric and Oceanic Technology*, *21*(7), 1059–1073.

Zibordi, G., Holben, B., Mélin, F., D'Alimonte, D., Berthon, J. -F., Slutsker, I., et al. (2010). AERONET-OC: An overview. *Canadian Journal of Remote Sensing*, *36*(5), 488–497.

Zibordi, G., Mélin, F., & Berthon, J. -F. (2006). Comparison of SeaWiFS, MODIS and MERIS radiometric products at a coastal site. *Geophysical Research Letters*, *33*, L06617.

Zibordi, G., Mélin, F., Berthon, J. -F., & Canuti, E. (2013). Assessment of MERIS ocean color data products for European seas. *Ocean Science Discussions*, *10*(1), 219–259.